



This is a repository copy of *Temporal and periodic analysis of penumbra–umbra ratio for the last four solar cycles*.

White Rose Research Online URL for this paper:

<https://eprints.whiterose.ac.uk/209365/>

Version: Published Version

Article:

Chowdhury, P., Kilcik, A. orcid.org/0000-0002-0094-1762, Saha, A. et al. (3 more authors) (2024) Temporal and periodic analysis of penumbra–umbra ratio for the last four solar cycles. *Solar Physics*, 299 (2). 19. ISSN 0038-0938

<https://doi.org/10.1007/s11207-024-02263-5>

Reuse

This article is distributed under the terms of the Creative Commons Attribution (CC BY) licence. This licence allows you to distribute, remix, tweak, and build upon the work, even commercially, as long as you credit the authors for the original work. More information and the full terms of the licence here:

<https://creativecommons.org/licenses/>

Takedown

If you consider content in White Rose Research Online to be in breach of UK law, please notify us by emailing eprints@whiterose.ac.uk including the URL of the record and the reason for the withdrawal request.



eprints@whiterose.ac.uk
<https://eprints.whiterose.ac.uk/>



Temporal and Periodic Analysis of Penumbra–Umbra Ratio for the Last Four Solar Cycles

Partha Chowdhury¹ · Ali Kilcik²  · Ankit Saha³ · Jean-Pierre Rozelot⁴ · Vladimir Obridko^{5,6} · Robertus Erdélyi^{7,8,9}

Received: 17 July 2023 / Accepted: 26 January 2024
© The Author(s) 2024

Abstract

We investigate the long-term dynamic behavior of the sunspot penumbra to umbra area ratio by analyzing the Debrecen Photoheliographic Data (DPD) of sunspot groups during the period 1976–2017 (Solar Cycles 21–24). We consider all types of spots and find that the average penumbra–umbra ratio does not exhibit any significant variation with spot latitudes, solar-cycle phases as well as sunspot-cycle strengths. However, the behavior of this ratio is different when we consider the latitudinal distribution of the northern and southern hemispheres separately. Our analysis indicates that for daily total sunspot area the average spot ratio varies from 5.5 to 6.5 and for very large sunspots ($> 5000 \mu\text{Hem}$; one μHem is 10^{-6} the area of visual solar hemisphere) its value rises to about 8.3. In the case of the group-sunspot area, the average spot ratio is ~ 6.76 . Furthermore, we found that this ratio exhibits a trend for both smaller (area $< 100 \mu\text{Hem}$) and large (area $> 100 \mu\text{Hem}$) sunspots. Finally, we report the periodic and quasiperiodic variations present in this ratio time series after applying the multitaper method (MTM) and Morlet-wavelet technique. We found that along with the ~ 11 -year solar-cycle period, the penumbra to umbra area ratio also shows several midterm variations, specifically, Rieger-type and quasibiennial periodicities. We also found that Rieger-type periods occur in all cycles, but the temporal evolution and the modulation of these types of periodicities are different in different solar cycles.

Keywords Sunspot: umbra · Sunspot: penumbra · Solar cycle · Wavelet analysis · Periodicity · Sunspots

1. Introduction

Sunspots are defined as dark regions observed on the solar disk in white light where the magnetic field is concentrated and therefore they are cooler than their surroundings. It is well known that a sunspot consists of two parts: the central dark part of the sunspot is called the umbra and the relatively lighter region surrounding the umbra is the penumbra (see, for example, Bray and Loughhead, 1964). Both parts have different physical properties such as magnetic-field strength, temperature, fine structures, etc. The magnetic nature of sunspots has been known for more than a hundred years beginning with the pioneering work of George Ellery Hale in 1908 (see also, for example, Jurčák et al., 2017). The umbra has

Extended author information available on the last page of the article

stronger magnetic fields compared to the penumbra and the strength of the magnetic field decreases with the radial distance from the umbral core (see, for example, Borrero and Ichimoto, 2011). Umbral- and penumbral-area measurements of sunspots may give information about their magnetic field (Solanki, Inhester, and Schüssler, 2006; Hathaway, 2015). Thus, an investigation of the umbra–penumbra area of sunspots may help to better understand the magnetic structure of sunspots, as well as enable new insight into the processes of the solar dynamo and also solar activity.

The ratio between the sunspot penumbra and umbra areas has been investigated by various authors for a long time (e.g., Nicholson, 1933; Waldmeier, 1939; Jensen, Nordø, and Ringnes, 1955; Antalová, 1971; Brandt, Schmidt, and Steinegger, 1990; Vaquero et al., 2005; Hathaway, 2013; Carrasco et al., 2018; Jha, Mandal, and Banerjee, 2019). The earliest studies suggested an almost constant umbra and penumbra area ratio; Nicholson (1933) reported that the umbra–penumbra area ratio is about 0.21 from data of the Royal Observatory, Greenwich (RGO) covering the time interval 1917 to 1920. He used only unipolar sunspots or the preceding spot in a sunspot group. Waldmeier (1939) reported the umbra–penumbra area ratio as 0.42 and noted that the ratio decreases with increasing sunspot area. Jensen, Nordø, and Ringnes (1955) analyzed 653 single and regular sunspots with areas larger than 100 millionths of a solar hemisphere (μHem) for 1878 to 1945, obtained from the RGO, and found that the umbra–penumbra area ratio is 0.23. They found that the ratio is a function of sunspot area and the phase of the 11-year solar cycle. These conclusions were corroborated by Tandberg-Hanssen (1955, 1956) and are applicable to bipolar and complex groups.

Bray and Loughhead (1964) critically reviewed these studies and pointed to a significant inconsistency and unreliability of the results obtained. They used the index

$$q_1 = A_u/A_w, \quad (1)$$

where A_u is the area of the umbra and A_w is the total area of the entire sunspot group. Bray and Loughhead (1964) noted that the average value of q_1 decreases at the maximum of the sunspot cycle. On average, q_1 is equal to 0.17 with a large spread of individual values. Previously, Waldmeier (1939) showed that q_1 increases with the spot area. This result contradicts the findings of Jensen, Nordø, and Ringnes (1955). Bray and Loughhead (1964) chose not to touch on this issue at all in their review.

Antalová (1971, 1991) conducted a study of the relative area of the umbra for a period of 85 years (1874–1959). It turned out that this value exhibits rather significant variations, with the smallest value in Cycle 14. As a rule, this index was less at the maxima than at the minima of the activity cycles. These results are consistent with the findings of Jensen, Nordø, and Ringnes (1955) and Tandberg-Hanssen (1955). In addition, this index for large spots is less than for small ones, see Antalová (1971). Later, Brandt, Schmidt, and Steinegger (1990) analyzed 126 sunspots around the maximum of the solar activity in 1980 and they found that the umbra–penumbra area ratios were 0.24 for small sunspots (for total areas around 50 μHem) and 0.32 for large ones. Vaquero et al. (2005) found that the umbra–penumbra ratio was around 0.25 from the sunspot observations made during the 1862–1866 period (declining phase of Solar Cycle 10 up to its minimum).

According to Hathaway, Wilson, and Campbell (2007) the mean value of relative umbra area is equal to 0.2. With an increase in the average spot area, this index will decrease. The cyclic dependence of the index is weak, and there was no dependence on latitude. For small sunspot groups, this index showed strong variations between 1910 and 1950. This result was later confirmed by Bludova, Obridko, and Badalyan (2014).

Detailed analyses of the sunspot umbra–penumbra area ratio were presented by Hathaway (2013) and Jha, Mandal, and Banerjee (2019). Hathaway (2013) used data from the

RGO for more than 100 years (1874–1976). He found that the penumbra to umbra area ratio did not depend on the heliographic latitude of the sunspots and the phase of the cycle. He also found that the umbra–penumbra area ratio of small groups (smaller than $100 \mu\text{Hem}$) shows a systematic change with time. Jha, Mandal, and Banerjee (2019) studied the sunspot penumbra to umbra area ratio using Kodaikanal data from 1923 to 2011 (Cycles 16–23). They found that the average umbra–penumbra area ratio varies with sunspot size correspondingly, while the ratio has not shown any dependencies on heliographic latitude, cycle phase, and cycle amplitude.

Bludova, Obridko, and Badalyan (2014) showed that the smallest groups with an area of less than $100 \mu\text{Hem}$ make the greatest contribution to the time variation of q_1 .

In this study, we investigate the long-term dynamic behavior of the sunspot penumbra to umbra area ratio by analyzing the Debrecen Photoheliographic Data (DPD) of the period 1976–2017 (Solar Cycle 21–24). We focus on the temporal and periodic behaviors of the ratio for northern and southern hemispheres of the Sun, respectively. Time profiles and periodicity analyses are used to describe the ratios' long-term dynamic behavior in detail. Section 2 contains the data and methodology, Section 3 the analysis and results, and Section 4 the discussion and conclusions.

2. Observational Data

We used the data of the daily individual sunspot groups obtained at the Debrecen Photoheliographic Data (DPD) sunspot catalog (Baranyi, Györi, and Ludmány, 2016) from June 1976 until December 2017, covering the complete Solar Cycles 21 to 23 and a major part of Cycle 24. The DPD sunspot catalog is mainly based on solar images taken at Gyula (recently known as Gyula Bay Zoltan Solar Observatory, GSO, *hspf.eu/*) and Debrecen Heliophysical Observatory (DHO) (Györi, Baranyi, and Ludmány, 2011). The gaps present in the observations were filled in by white-light images taken by different observatories from all over the world. From 1976, the sunspot database of the Royal Observatory, Greenwich (RGO) was replaced by the DPD sunspot catalog. In both the above-mentioned observatories forming a DPD catalog, measurements were made by white-light full-disk photographic observations and the archive consists of more than 150,000 digitized plates. This catalog contains the date and time of observation, heliographic latitude [λ] and longitude [L], corrected whole-spot area [A_w], hereafter sunspot area, corrected umbral area [A_U], and central meridian distance [CMD], etc., of all the observed sunspot groups on daily basis. Along with these, the DPD catalog covers information about the penumbra region of each identified sunspot, with corrected projection effects. The main components of any stable sunspot are the umbra and the penumbra. Although it is known that the sunspots photometric and magnetic boundaries do not coincide, Obridko et al. (2022) investigated sharp structures visible in solar magnetic-field tracers. Relying on the fact that the magnetic boundary is not defined with sufficient precision, they showed that the photometric and magnetic properties of structures at the solar surface need further investigations, and certainly through the leptocline (see Kosovichev and Rozelot, 2018, for definition). To compile the DPD sunspot catalog, a software program package SAM (Sunspot Automatic Measurement) was developed that automatically determines the contours characterizing the umbra–penumbra and the photosphere penumbra boundaries thorough which umbral and penumbral areas and the heliographic positions of the spots are measured from the images (see Györi, 1998, 2005, for details). In this process, based only on the intensity the darker portion of the spot is considered as an umbra. The

unit of the corrected area of the whole spot and the umbra is a millionth of a solar hemisphere [μHem]. In this catalog, the umbral area is taken as 0 when its area is $< 0.5 \mu\text{Hem}$. Here, the umbra area is defined as the total area of the umbra of all the sunspots in a group rather than the area of the umbra of an isolated spot. A zero umbral area indicates that either the derived A_u is $< 0.5 \mu\text{Hem}$ or the internal pattern of the spot is not identified properly (Baranyi, Győri, and Ludmány, 2016). The active regions (ARs) consisting of pores and zero umbra area were not considered in the present investigation. Our observation covered a total of 12,336 days sunspots observations. These datasets are publicly available at the website fenyi.solarobs.unideb.hu/pub/DPD/. More information about the DPD catalog and the relevant datasets can be found in Baranyi, Győri, and Ludmány (2016), and Győri, Ludmány, and Baranyi (2017).

The ratio (q) of the penumbral area to the umbral area of any sunspot is defined as:

$$q = (A_w/A_u) - 1, \quad (2)$$

where, A_w and A_u are the sunspot area and umbra area, respectively, with units of μHem . Both of these parameters were corrected for foreshortening based on the positions of sunspots between the disk center and the limb. A similar definition of this ratio was considered by Hathaway (2013) and Carrasco et al. (2018).

Note that this definition of q differs from the definition of q_1 adopted in a number of other papers and discussed above in the Introduction, so that an increase in q_1 corresponds to a decrease in q and vice versa.

3. Results

We determine the ratio q for the period June 1976–December 2017 from the DPD catalog that covers the Solar Cycles 21 to 24. Different aspects of this ratio are discussed in this section.

3.1. Variation of the Penumbra–Umbra Area Ratio with Sunspot Area

We have studied the overall behavior of this ratio (q) with respect to the size of the sunspot observation in the DPD database for the entire time period under investigation. For this purpose, the data are grouped according to their corrected full sunspot area into bin sizes of $50 \mu\text{Hem}$ between 50 and $\sim 7500 \mu\text{Hem}$ and we calculated the average ratio (q_{avg}) for all sunspots lying in that particular bin. Figure 1 represents q_{avg} as a function of the daily total sunspot area (upper panel) and total group-sunspot area (lower panel). The red-dotted regions delimit the standard error of 2σ uncertainty. The upper panel shows the variation of the penumbra to umbra area ratio with respect to the daily total sunspot area in the full solar disk. The daily total area is the sum of the areas of each spot present in a group in each day. The daily total umbral area is also the sum of all sunspot umbra areas for each day. Figure 1 indicates that this ratio begins with the value ~ 6.4 , then falls to 5.5 for the size $\sim 100 \mu\text{Hem}$, and becomes almost flat at the value ~ 6 for the size from $\sim 700 \mu\text{Hem}$ to $\sim 4500 \mu\text{Hem}$ with two spikes (local maxima) having values ~ 6.3 and ~ 7 when the sunspot area becomes the size of $\sim 500 \mu\text{Hem}$ and $\sim 5500 \mu\text{Hem}$, respectively.

This slow upward trends of the ratio indicates that larger sunspots tend to have a larger penumbra. Figure 1 exhibits that the ratio has an average value ~ 6 till the value of the sunspot area $\sim 5000 \mu\text{Hem}$. This q_{avg} shows variation between 5.5 and 8.7 when the daily

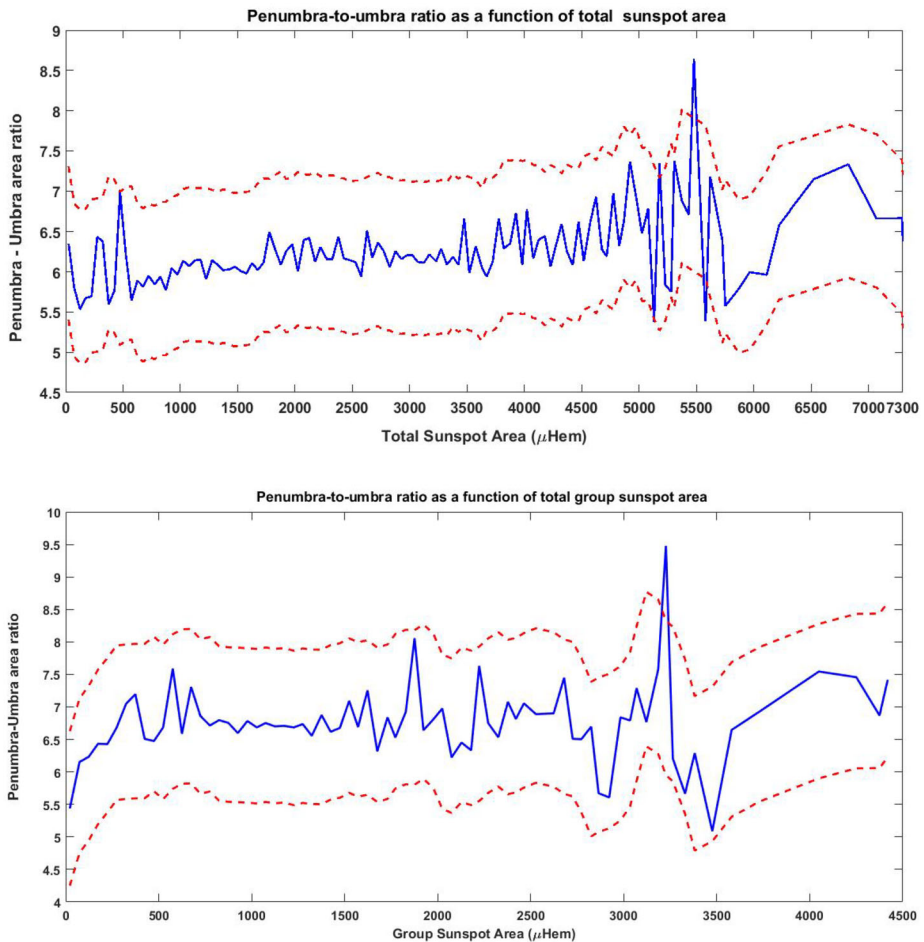


Figure 1 Penumbra to umbra area ratio as a function of daily total sunspot area (upper panel) binned over $50 \mu\text{Hem}$ and penumbra to umbra area ratio as a function of total group-sunspot area (lower panel). Red shaded regions represent the 2σ error.

total sunspot area acquires the very high values from $5000 \mu\text{Hem}$ to $7500 \mu\text{Hem}$. It is possible that this fluctuating character is simply due to the fact that sunspot areas $> 4500 \mu\text{Hem}$ are very few in number ($\sim 1\%$) with smaller umbra area. We have found that the error region above sunspot area $\geq 5000 \mu\text{Hem}$ are considerably larger and most probably arose due to the poor statistics in those bins. On the other hand, a strong scatter of values for small sunspot areas can be associated with inaccuracies in determining areas or the groups with rudimentary penumbra. We have also calculated the necessary statistical parameters for all data displayed in Figure 1. The mean value, standard deviation, and standard error of the q_{avg} plots Figure 1(a) are 6.266, 0.452, and 0.0408, respectively.

Figure 1, lower panel, shows the variation of the penumbra to umbra area ratio with respect to the whole group area for all sunspot groups observed during the above-mentioned time span. In this case, the bin size is also between 50 and $\sim 4500 \mu\text{Hem}$. This figure indicates that the ratio begins with the value ~ 5.5 , gradually rises to ~ 7 for the size ~ 380

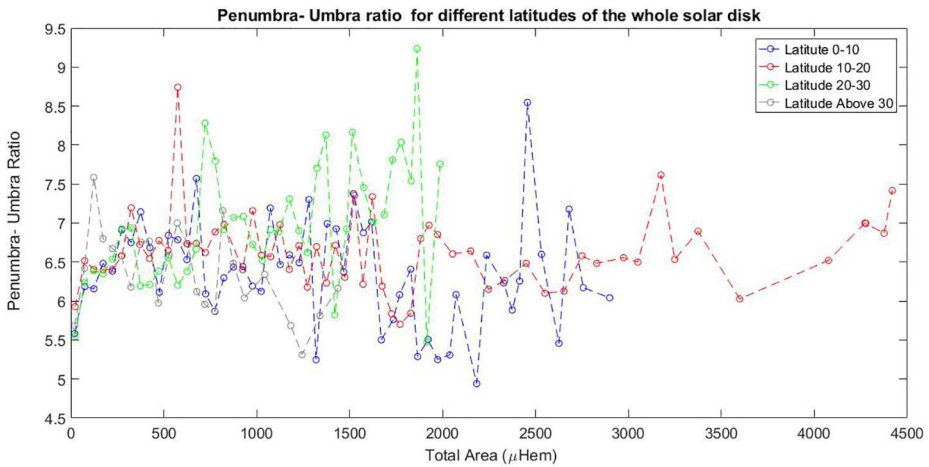


Figure 2 Variation of q_{avg} as a function of total total sunspot-group area in four different latitude bands of the full disk.

μHem , then falls to 6.5 for the size $\sim 500 \mu\text{Hem}$. The ratio showed two peaks having values ~ 7.6 and ~ 7.3 within $600 \mu\text{Hem}$ to $700 \mu\text{Hem}$. Then, the ratio took an average value of ~ 6.5 from $750 \mu\text{Hem}$ to $\sim 1800 \mu\text{Hem}$. Then, it showed some up and down nature varying between ~ 8.3 and ~ 5.6 within the zone $\sim 3000 \mu\text{Hem}$. The ratio showed its highest value ~ 9.5 and lowest value ~ 5 when the group-sunspot area is $\sim 3300 \mu\text{Hem}$ and $\sim 3500 \mu\text{Hem}$, respectively. In the small-area regions ($\leq 2000 \mu\text{Hem}$), spikes were formed as there are some sunspot groups having relatively small umbra areas. We assume the strong peak and downfall of the ratio after $2500 \mu\text{Hem}$ is produced due to the presence of a very small number of groups ($\sim 0.2\%$) that belong to those bins. The mean value, standard deviation, and standard error of the data displayed in the lower panel of Figure 1 are 6.761, 0.594, and 0.069, respectively.

3.2. Variation of the Penumbra–Umbra Area Ratio with Latitude

According to the “sunspot butterfly diagram”, only a few sunspots are observed at high latitude during the onset of a new cycle and gradually their number increases and they appear at lower latitudes in the course of solar-cycle progression. We examined possible variations of q_{avg} with latitude by calculating this quantity for sunspot groups in four latitude bands, 0° to 10° , 10° to 20° , 20° to 30° , and $> 30^\circ$ following Hathaway (2013). First, we considered the two opposite hemispheres together (full solar disk) and the results are shown in Figure 2. This figure shows the variation of q_{avg} as a function of total group-sunspot area in four different latitude bands. Although we have found that the majority of the sunspot groups ($\sim 90\%$) belong to $10 \mu\text{Hem}$ to $1000 \mu\text{Hem}$ and only a very small fraction ($\sim 1\%$) exceed the size $> 2000 \mu\text{Hem}$, to obtain an overall clear picture, we have considered the sunspot groups $> 2000 \mu\text{Hem}$ in our analysis.

From these plots, we observe that the value of ratio starts from ~ 5.5 to ~ 6 in different latitude bands. These figures indicate a large scatter in the values of q_{avg} in all latitude bands without any exception. We found that variations in the value of q_{avg} do not depend on the position of the spots in different latitudes. This result is consistent with those of Hathaway (2013) and Jha, Mandal, and Banerjee (2019). Table 1 represents some statistical properties

Table 1 Some statistical properties of q_{avg} in different latitudes for the whole solar disk.

Latitude [°]	Mean	Median	Standard Deviation	Standard Error
0–10	6.367	6.382	0.6770	0.093
10–20	6.631	6.579	0.4866	0.063
20–30	6.967	6.916	0.7874	0.124
>30	6.361	6.379	0.5324	0.108

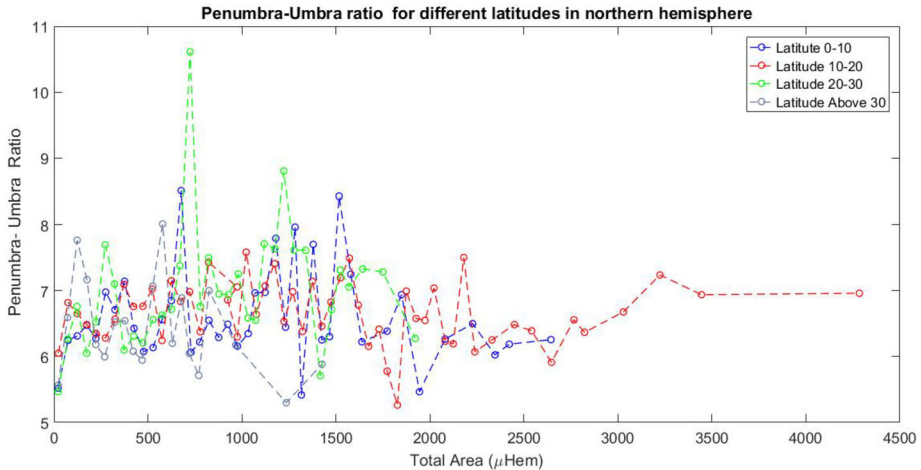


Figure 3 Same as Figure 2 but for the Northern hemisphere.

of q_{avg} in different latitude bands. To examine the variations of q_{avg} in the two hemispheres separately, we have divided the full sunspot-group area data in + and – latitudes groups. The latitudes in the + groups are considered as northern hemisphere and the – latitudes are treated as the southern hemisphere. In both cases, the datasets were, again, divided into four latitude bands, i.e., 0° to 10°, 10° to 20°, 20° to 30°, and > 30° as previously seen (Hathaway, 2013).

Figure 3 represents the variations of q_{avg} in the northern hemisphere in the different latitudes. For all latitudes, its value starts from 5.5–6 and then shows a scattering behavior.

Variations of q_{avg} in the southern hemisphere at different latitudes are displayed in Figure 4. In this hemisphere, for small sunspot-group area, q_{avg} starts from ~5.6 to ~6.2 for different latitudes. The scattering behaviors of q_{avg} at different latitudes are also found in this hemisphere. Table 2 represents some statistical properties of q_{avg} in the opposite hemispheres in different latitudes.

From the above-mentioned graphs, it is clear that q_{avg} does not exhibit any particular trend in any of the hemispheres as well as the full solar disk and hence we may conclude that this ratio is independent of the latitude distribution of a spot (Antalová, 1971; Hathaway, 2013; Jha, Mandal, and Banerjee, 2019; Hou et al., 2022; Takalo, 2023).

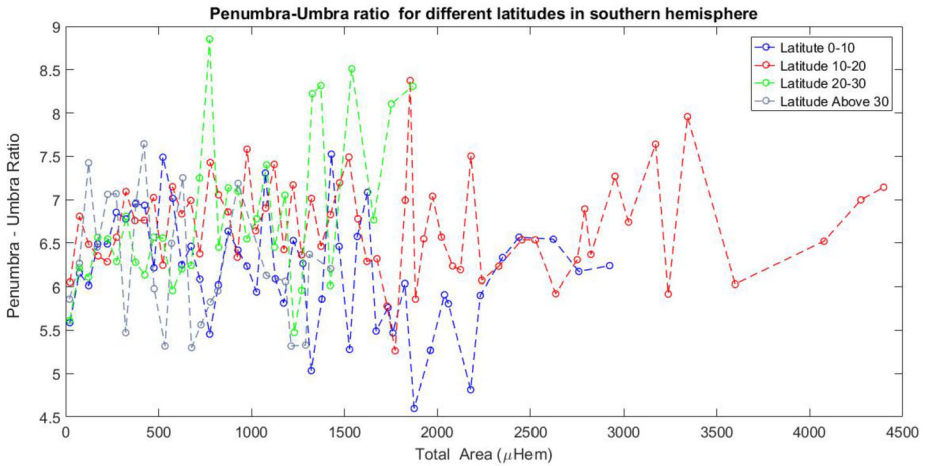


Figure 4 Same as Figure 2 but for the Southern hemisphere.

Table 2 Some statistical properties of q_{avg} in different latitudes and hemispheres.

Latitude [°]	Mean	Median	Standard Deviation	Standard Error
Northern Hemisphere				
0–10	6.587	6.385	0.697	0.109
10–20	6.674	6.651	0.468	0.063
20–30	6.999	6.849	0.926	0.158
>30	6.432	6.192	0.708	0.158
Southern Hemisphere				
0–10	6.191	6.223	0.644	0.093
10–20	6.705	6.691	0.556	0.070
20–30	6.811	6.557	0.874	0.152
>30	6.270	6.154	0.730	0.149

3.3. Variations with Solar-Cycle Phase and Different Cycle Amplitude

In this section, we investigate the variations of q_{avg} during the different phases of the investigated solar cycles, like ascending, maximum, descending, and minimum phase, of all the cycles separately. We have defined each of these phases following Hathaway (2013). We are also motivated by some of the earlier studies like Jensen, Nordø, and Ringnes (1955), Tandberg-Hanssen (1956), Antalová (1971), Hathaway (2013) to perform this analysis in the recent solar cycles where these authors reported different values of q_{avg} during a cycle-minima phase as opposed to a cycle-maximum phase. The variations of q_{avg} during different phases of the Solar Cycles 21–24 are displayed in Figures 5(a)–(d). From these figures it is evident that during Cycle 21, q_{avg} values vary between 2.2 and 11 for very small sunspot areas (smaller than 500 μHem) and cluster mainly within the interval 4 to 6 for all branches of the cycle. However, for Cycle 22 during the above-mentioned phase q_{avg} was concentrated within 5 to 6 up to sunspot areas of 500 μHem and for large sunspot areas (1000–3000 μHem) its value varies between 5.8 and 7. In the case of Cycle 23, during the rising branch,

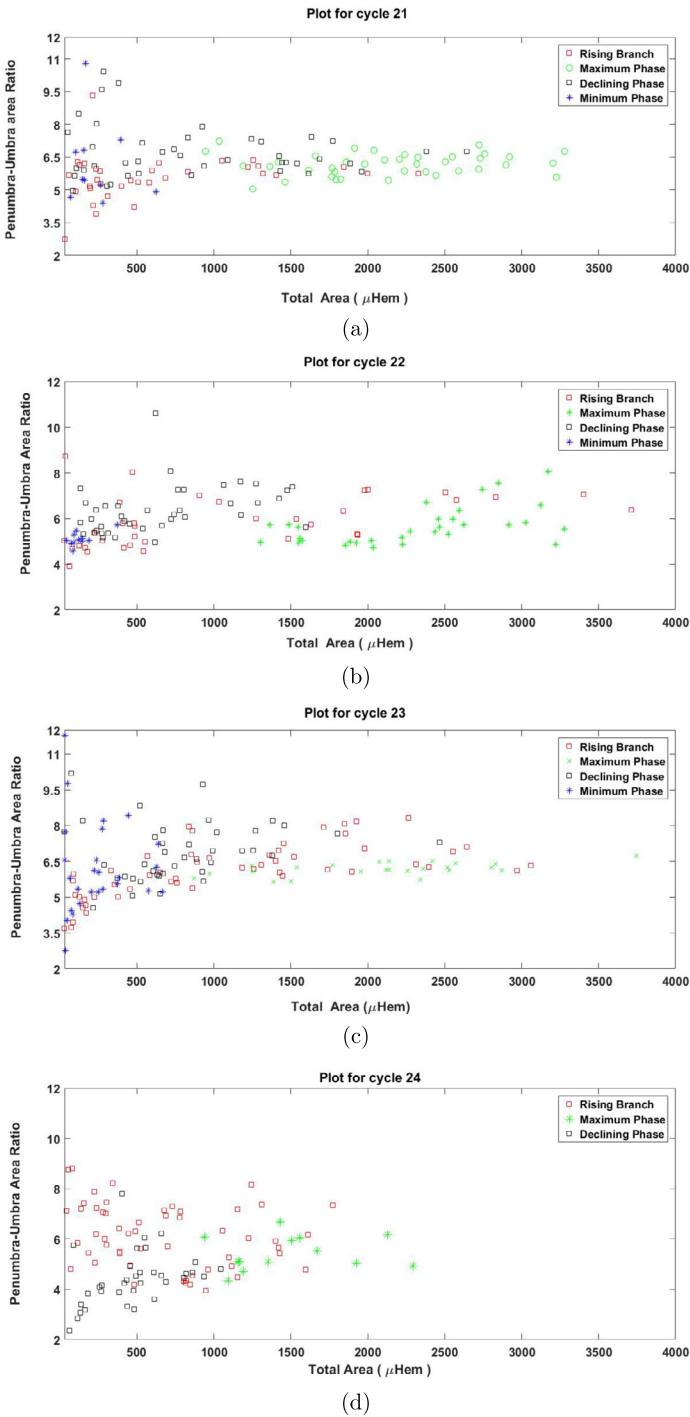


Figure 5 Panel (a) to (d): Variation of q_{avg} as a function of total group-sunspot area in four different activity phases of the solar cycles as written on the panel.

q_{avg} varies from 4 to 6.5 for sunspot areas up to $500 \mu\text{Hem}$, for large sunspot areas q_{avg} value shows ups and downs with an average value of ~ 6 . For Solar Cycle 24, the q_{avg} value was scattered between 2 to 8.2 within small sunspot-group areas of $500 \mu\text{Hem}$ and demonstrated a varying nature from 4 to 8 for large sunspot areas.

The maximum phase of any solar cycle usually persists for 2–3 years with the appearance of large sunspots. During Cycle 21, q_{avg} maintains an average value ~ 6 during this episode. For Cycle 22, this value varies between 5 and 8. For Cycle 23, it maintains a value ~ 6 and from 4–6 in the case of Cycle 24.

During the descending and minimum phases of any cycle, solar activities are less prominent and the sunspot numbers decrease gradually. Sunspot areas also exhibit smaller sizes. Here, we studied some properties of q_{avg} during these two phases for Cycles 21–24, for visualization see Figures 5(a)–(d). For Cycle 21, during the decay phase, q_{avg} takes a value between 5 and 10.2 for sunspot areas of $\leq 500 \mu\text{Hem}$. For sunspot areas $> 500 \mu\text{Hem}$, it possesses a value from 6 to 7. During the minimum phase its value q_{avg} varies from 4.2 to 10.2. At the time of the descending phase of Cycle 22, q_{avg} has values from 5 to 8 (except one point) and about 5 during the minimum phase. In the case of Cycle 23, q_{avg} is scattered between 4.8 and 10 during the descending phase and between 2.5 to 12 at the minimum phase with a concentration around 6. Our study covers the entire descending phase of Cycle 24. The value of q_{avg} changes from 2 to ~ 8 with a concentration within the zone 4 to 6.

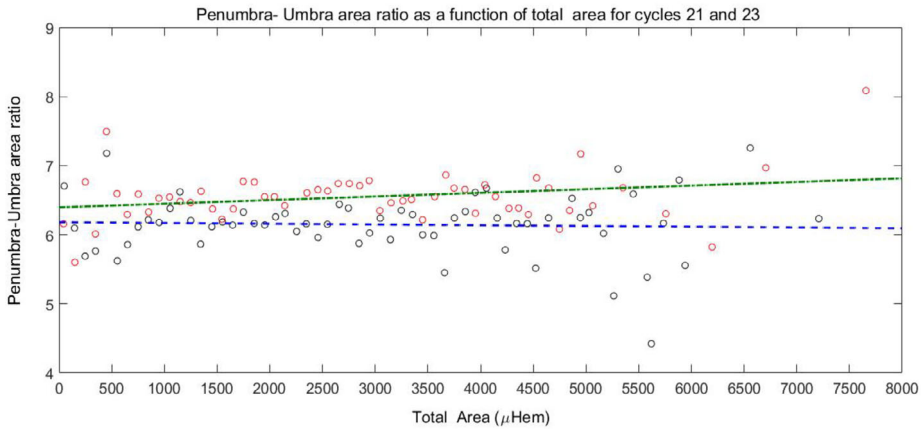
The value of q_{avg} may vary in different solar cycles and to investigate the overall dependency of this quantity we have examined the variations in q_{avg} as recorded for each solar cycle under investigation. Figure 6(a) represents the variations in q_{avg} as a function of sunspot area for Cycles 21 and 23. During Cycles 21 and 23, for sunspot area up to $5000 \mu\text{Hem}$, q_{avg} mainly clusters within the range of 5.5 to 6.5 values. For very large sunspot areas ($> 5000 \mu\text{Hem}$) q_{avg} shows a large scatter and its value varies from 5 to 8 for both the cycles under study. The mean values of q_{avg} for Solar Cycles 21 and 23 are ~ 6.14 and ~ 6.54 , respectively.

Variations in q_{avg} as a function of sunspot area for Solar Cycles 22 and 24 are shown in Figure 6(b). To see the trend of penumbra–umbra area with respect to the total sunspot area we added linear fits for each cycle data (Chowdhury et al., 2022). In both these cycles the q_{avg} lies mainly within the range of 5 to 6. It is observed that the average values of q_{avg} for even-numbered Cycles 22 and 24 were ~ 6.16 and ~ 5.55 , respectively. The variations of q_{avg} in different solar cycles may be due to different dynamic behavior of smaller and larger spots. Also, in contrast to the Cycles 21 and 23, there is a weakly increasing trend in q_{avg} values with sunspot area. Table 3 illustrates some of the statistical properties of Figures 6(a) and (b).

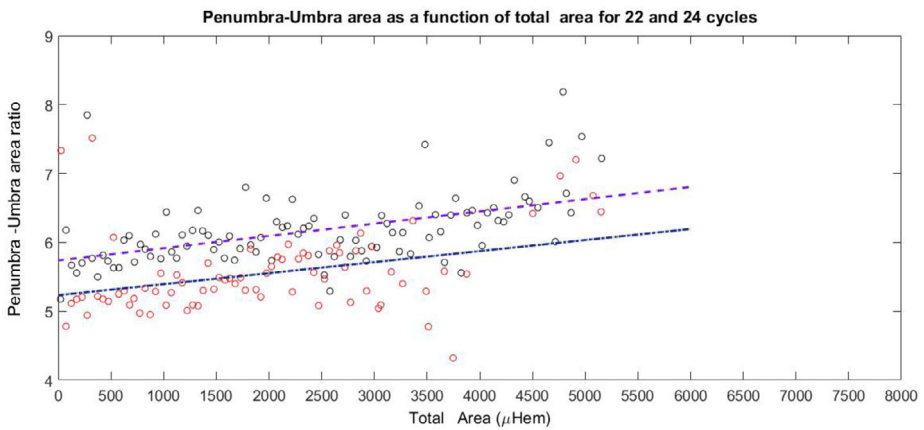
3.4. Dynamic Behavior of Smaller and Larger Spots and Other Properties

It is well known that sunspots of different sizes exhibit different types of behavior in the course of a solar cycle (Gao, Li, and Li, 2017). In this section, we study the evolution of q for two classes of sunspots: i) sunspot groups with areas $\leq 100 \mu\text{Hem}$ (small sunspot groups) and (ii) sunspot groups with areas $> 100 \mu\text{Hem}$ (medium to large sunspot groups). We have considered this threshold value at $100 \mu\text{Hem}$ due to the fact that we see a dip in the value of q at this area in Figures 1(a) and (b). For this purpose, we have calculated the average value of q on a yearly basis for both sunspot categories.

Figure 7 shows the three-yearly averages of the q for small (areas $\leq 100 \mu\text{Hem}$) and large sunspot groups (areas $> 100 \mu\text{Hem}$). It is found that q values vary between 2.8 (in 2017) and 8.6 (in 2003) for small groups and they vary between 4 (in 2016) and 8.3 (in



(a)



(b)

Figure 6 Penumbra-to-umbra area ratio as a function of total sunspot area at various phases of the sunspot cycle indicated by the different symbols with regression plots. (a) Cycles 21 and 23, (b) Cycles 22 and 24.

Table 3 Some statistical properties of *q* values for the investigated cycles.

Cycle no	Mean	Median	Standard Deviation	Standard Error
21	6.147	6.166	0.451	0.057
22	6.170	6.100	0.508	0.051
23	6.549	6.550	0.366	0.049
24	5.550	5.410	0.579	0.066

2008) for large groups during the investigated time period. They have a tendency to follow the sunspot cycle with some differences; i) the amplitude of variation is quite small during Cycle 22 for small groups compared to large ones, ii) the amplitude of variation decreased markedly during solar Cycle 24 for both categories, iii) contrary to small groups, the cyclic

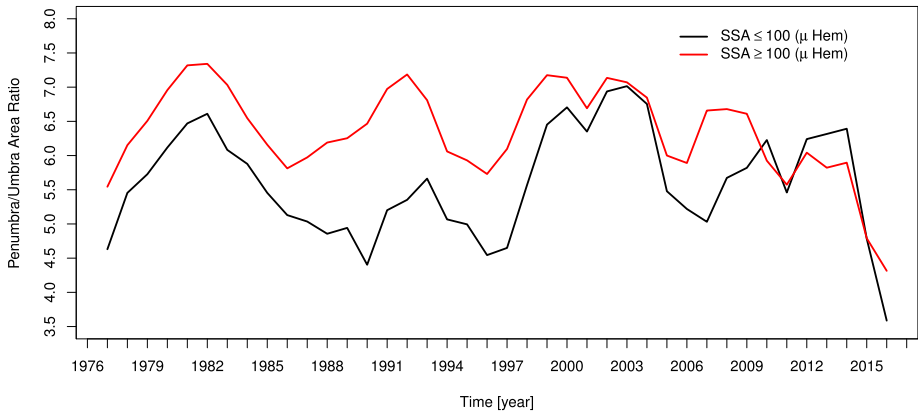


Figure 7 Temporal variation of the annual q values computed for Cycles 21–24 records in two categories.

variation is not clearly seen in the case of large groups during Solar Cycle 24. In the case of the sunspot groups with areas $\leq 100 \mu\text{Hem}$, we have noted the sudden drop during 2000–2001 as well as 2010–2011. If we consider sunspot groups with areas $> 100 \mu\text{Hem}$, such a drop is observed during the period ~ 2000 –2001 and ~ 2014 . Perhaps these decreases of sunspot area are related with the Gnevyshev gap (GG) (Gnevyshev, 1967).

The monthly mean values of q , considering all types of sunspot groups were calculated for each year from 1976 to 2017 and are displayed along with the 13-month moving average in Figure 8. This figure indicates that during Cycle 21, the values of q lie mainly around the vicinity of 6. After this cycle, monthly q values show a rise and fall nature and follow characteristic solar-cycle properties. From the fitted curve, it is clear that during the deep minimum phase of Cycle 23, the value of q varied from 5 to 5.5, i.e., the value did not reduce much, although it has been reported that both sunspot number and area were abnormally lowered down in this time period (Hathaway, 2015). For comparison, we have plotted monthly and 13-month moving average of the International Sunspot Number of the full solar disk for the aforesaid period.

From Figure 8, it is also clear that the value of q varies during the course of a solar cycle. We have investigated the number distribution of q for all the solar cycles as well as different cycles, separately, under a study considering the monthly average value of q . Figure 9 presents the histogram plots of the number distribution of q . For Cycle 21 the maximum value of q lies within 6 to 7. The mean q -value for the Cycle 21 is 6.20 (standard deviation, $\text{std} = 1.14$). For Cycle 22 the histogram exhibits a maximum within 5 to 6. The mean q -value for the Cycle 22 is 5.92 (standard deviation, $\text{std} = 1.04$). In the case of Solar Cycle 23, q exhibits its maximum within 6 to 7. For this cycle, the average q -value is 6.30 (standard deviation, $\text{std} = 1.51$). The histogram peak has a maximum within 4 to 5 during Cycle 24 with average q -value 5.53 (standard deviation, $\text{std} = 1.83$). When all the solar cycles are considered together, the histogram for q -values is a maximum within 5 to 7, the average q -value is 6.02 (standard deviation, $\text{std} = 1.43$), and it is concentrated mainly within the zone 4 to 8. These plots show that the maxima of the penumbra–umbra area ratio changes from cycle to cycle due to the different strength of the solar cycles and therefore the sunspot areas (particularly the number of larger groups) are also different.

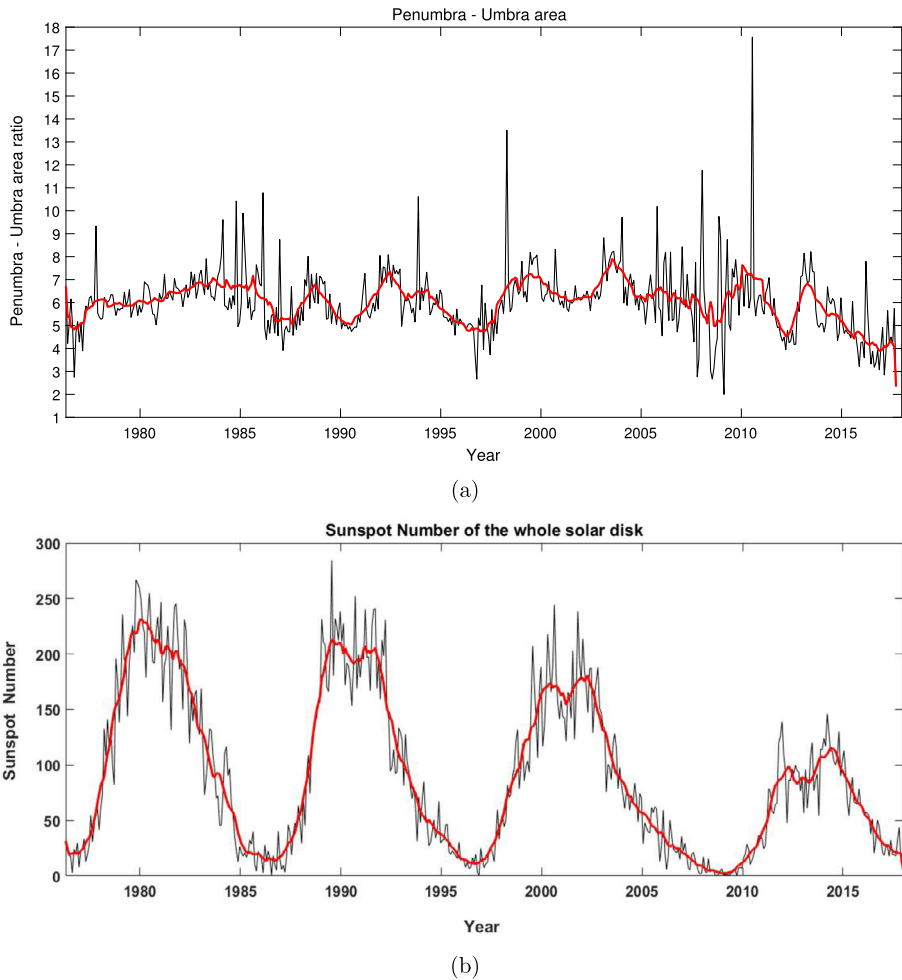


Figure 8 (a) Monthly (black) and 13-month smoothed (red) penumbra–umbra area ratio for Cycles 21–24 (b) Monthly (black) and 13-month smoothed (red) international sunspot number of the whole solar disk for Cycles 21–24.

3.5. Periodic and Quasiperiodic Variations of Penumbra–Umbra Area Ratio (q)

3.5.1. Methods

Figure 8 indicates that the ratio (q) exhibits fluctuations and follows a cyclic pattern of about 11 years, with different dynamical behavior in different sunspot cycles. Periodic and quasiperiodic variations in the different solar-activity indices like sunspot number/area, plage areas, 10.7 cm radio flux, $H\alpha$ flare activity, coronal mass ejections, etc., on time scales shorter than the 11-year Schwabe cycle have also been reported by several authors (see Hathaway, 2015, for details). Detailed analysis of these short-term periodic variations may provide clues to understanding the basics of different solar activities (McIntosh et al., 2017; de Paula, Curto, and Oliver, 2022; Korsós et al., 2023). In this section, we are interested

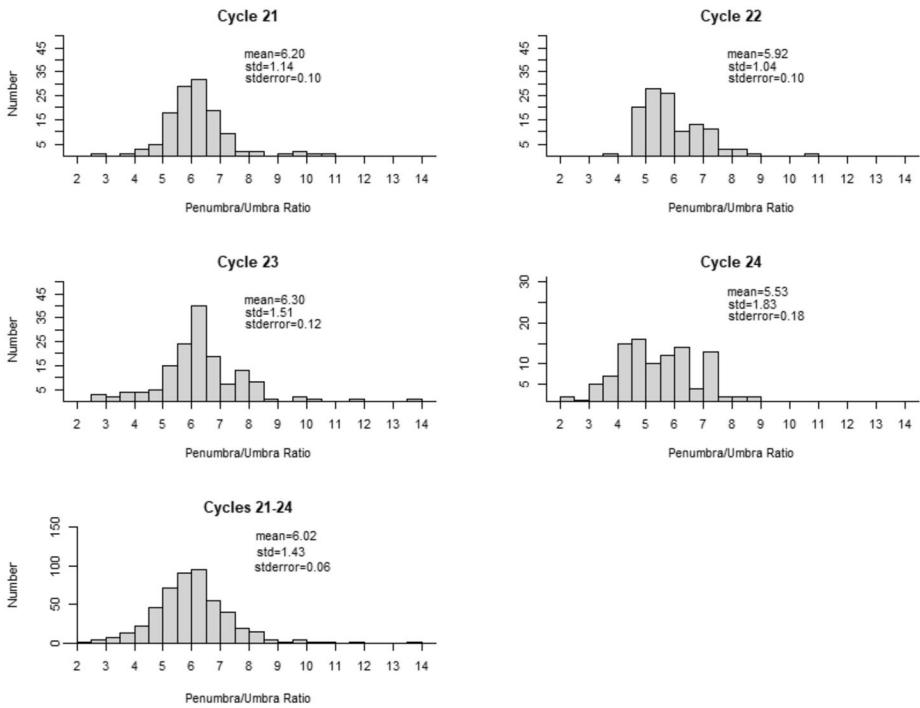


Figure 9 Histogram plot of penumbra–umbra ratio in different solar cycles and combining all cycles. The ratio is maximum in the zone of 5–7 when all cycles (Cycles 21–24) were considered.

in studying the periodic and quasiperiodic variations present in the monthly averaged value of q during the time period of investigation because this parameter (q) is directly connected with sunspot/solar magnetic-field activity. To determine the periodic variations present in the time series of q , we used both the multitaper method (MTM) (see Ghil et al., 2002, for more detail) and Morlet-wavelet analyses techniques with a red-noise background approximation (Torrence and Compo, 1998). The MTM is a very effective tool for finding low-amplitude harmonic oscillations that are highly statistically significant in the dataset, and it was widely used to evaluate various solar-activity indicators to determine what their periodic properties were (Di Matteo and Villante, 2017; Kilcik et al., 2018; Dobrica et al., 2018; Chowdhury et al., 2019; Kilcik et al., 2020; Ozguc et al., 2021; Ozguc, Kilcik, and Yurchyshyn, 2022; Korsós et al., 2023, and references therein). The MTM offers helpful tools for signal reconstruction (Park, 1992) and spectral estimate (Thomson, 1982; Percival and Walden, 1993) of a time series whose spectrum may include both broadband and line components. Ghil et al. (2002) include more detailed information on this technique. Here, three sinusoidal tapers were utilized, with frequency ranges selected between 0.004–0.5 (2–250 month) for the entire dataset and 0.16–0.25 (4–6.25 month) for the Rieger-period intervals. The noise spectrum assumed as a red spectrum. When the 95% confidence level is attained, we consider a signal to have been detected.

To investigate the temporal evolution of the periodicities present in the time series of q , we utilized the Morlet-wavelet analysis transform;

$$\Psi(\eta) = \pi^{-1/4} e^{i\omega_0 \eta} e^{-\eta^2/2}. \tag{3}$$

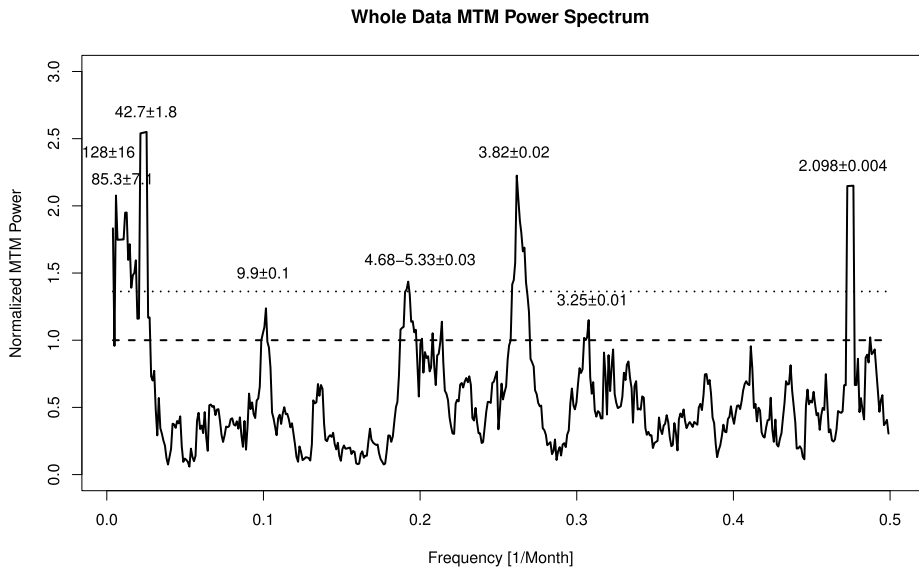


Figure 10 Periodic behavior of penumbra–umbra ratio with MTM tool. The numbers on top mark the detected periods and their possible errors in units of months.

Here, ω_0 is the nondimensional frequency and η represents nondimensional time. The wavelet analysis identifies periodic oscillations of time series in both time and frequency domains. For this time series, we have considered ω_0 as 6 and 12 for Rieger-type periods and other long-term periods, respectively (Torrence and Compo, 1998; Ravindra, Chowdhury, and Javaraiah, 2021; Ravindra et al., 2022; Chowdhury et al., 2022). In both cases, the bold dashed contours indicate the cone-of-influence (COI). We have considered a red-noise background (Torrence and Compo, 1998; Grinsted, Moore, and Jevrejeva, 2004) and the thin black contours inside the COI exhibit wavelet periods above 95% confidence level (Torrence and Compo, 1998; Grinsted, Moore, and Jevrejeva, 2004). We have also computed “global wavelet power spectra (GWPS)” that indicate time-averaged power in each case. Figures 10–12 represent the wavelet plots.

3.5.2. Results

Table 4 lists the intermediate term periodicities present in the time series of q as detected by the MTM method (see Figure 10).

Quasiperiodic variations in the monthly time series of q were investigated by using the MTM and Morlet-wavelet analysis techniques. The results are displayed in Figures 10, 11, and 12, respectively. Figure 11(a) indicates the presence of Rieger-type periodicities (130–190 days/4.3–6.3 months) in the dataset of q . Along with it, the well-known quasibiennial oscillations (QBOs) in the range of 1.2 year to 1.6 years (14.4 months to 19.2 months) (Bazilevskaya et al., 2014; Hathaway, 2015; Kiss and Erdélyi, 2018) were also detected and were concentrated in all solar cycles under study with varying lengths. Periods in the range of 2.5–3 years (30–36 months) appeared during Cycles 22, 23, and 24. Figure 12(a) indicates the presence of ~ 5 -year (~ 60 months) as well as ~ 11 -year (~ 132 months) periods (solar-cycle periodicity). Similar kinds of periods were also detected in the GWPS plots (see Figure 11(b) and Figure 12(b)).

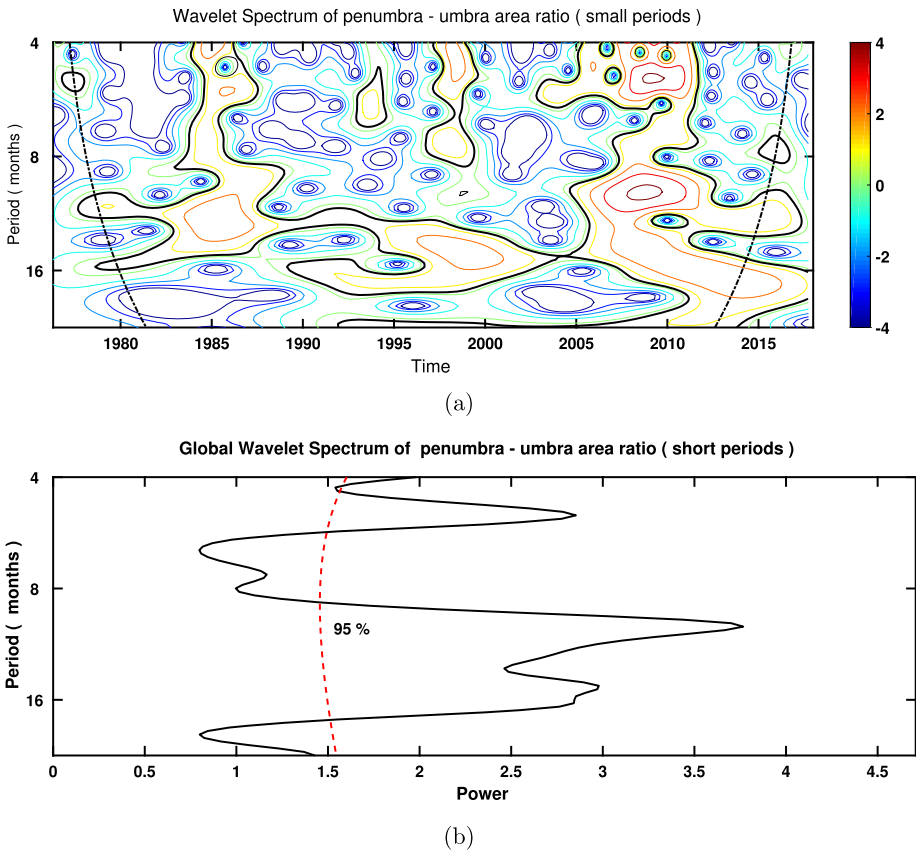


Figure 11 Panels a and b exhibit the local and global power spectra of the monthly mean penumbra–umbra ratio data series for the range 4–18 months. The 95% confidence level in GWPS is indicated by red dotted lines.

3.5.3. Evolution of Rieger-Type Periodicities

Rieger et al. (1984) reported the presence of a 154-day (5.13 months) periodic variation in solar hard-X- and γ -ray flare activity about the maximum phase of Cycle 21. Bogart and Bai (1985) studied the occurrence of flares inferred from microwave datasets for Cycles 19 to 21 and detected strong confirmation of a 152-day (5.07 months) periodicity. Later, these type of periods with varying length between 130–190 days (4.3–6.3 months) were detected in different solar and heliospheric activity indices, including asymmetry time series as well as in the galactic cosmic-ray datasets (Bai and Cliver, 1990; Bai and Sturrock, 1993; Carbonell and Ballester, 1992; Oliver, Ballester, and Baudin, 1998; Chowdhury, Khan, and Ray, 2009; Chowdhury et al., 2016, 2022; Knaack, Stenflo, and Berdyugina, 2005; Ravindra, Chowdhury, and Javaraiah, 2021; Ravindra et al., 2022; Kotz , 2021; Kors s et al., 2023) during different past solar cycles. These investigations suggest that Rieger-type periodicities are not only a feature of flare activity, but also connected with regions of compact magnetic-field structures. Gurgenchashvili et al. (2016) analyzed sunspot-area data for Cycles 14 to 24 and indicated that the Rieger group of periods are cycle dependent, i.e., shorter periods occur during stronger solar cycles. Lean (1990) indicated that the Rieger group of periods

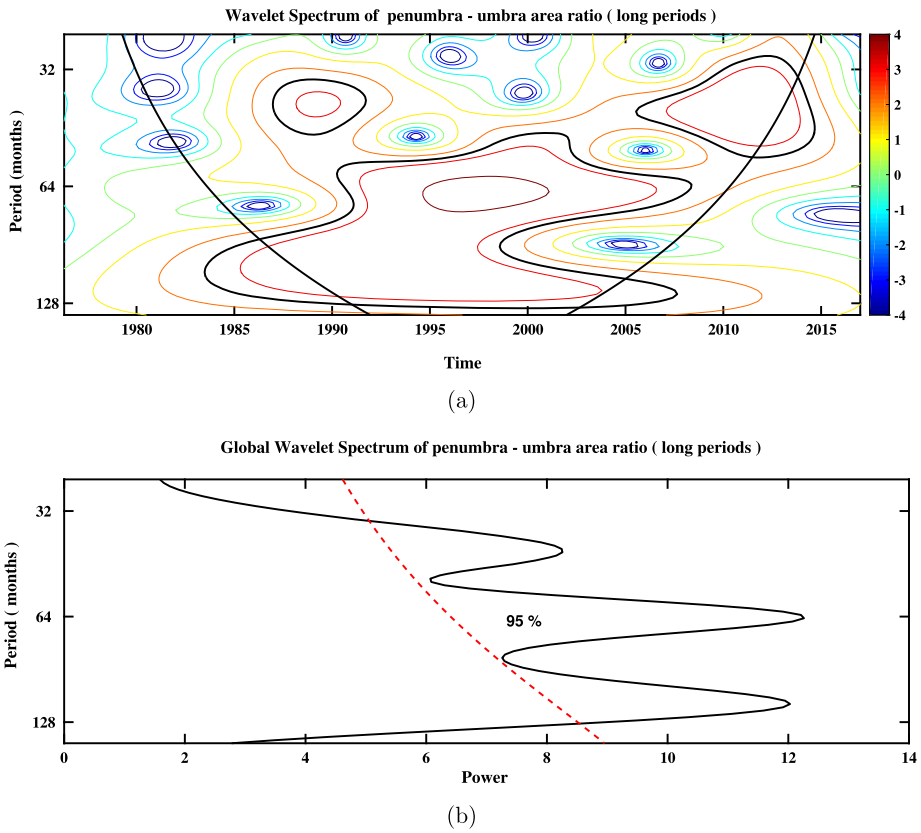


Figure 12 Panels a and b exhibit the global and local power spectra of the monthly mean penumbra–umbra ratio data series for the range 18–130 months. The 95% confidence level in GWPS is indicated by red dotted lines.

Table 4 Periods, with their errors, and period ranges determined using the MTM applied to q data for Solar Cycles 21 to 24.

Periods in months (> 95% confidence level)							
2.098 ± 0.004	3.25 ± 0.01	3.82 ± 0.02	$4.68-5.33 \pm 0.03$	9.9 ± 0.1	42.7 ± 1.8	85.3 ± 7.1	128 ± 16

are intermittent in nature and occurred mainly ~ 3 years (~ 36 months) during the solar-maximum activity.

Here, we have studied the nature and variations of the Rieger-type periodicities in the time series of q . To retrieve these periods, the dataset under study were processed through a simple passband filter that consists of 4 months and 7 months smoothing with a consequent subtraction of the latter data from the former one, following the recipe of Bazilevskaia et al. (2014, 2022). Next, we have applied the Morlet-wavelet tool to these extracted datasets considering $\omega_0 = 6$ under a “red-noise background” to explore the temporal evolution of Rieger-type periods. To see these periods in more detail we applied the MTM technique and

the frequency interval was chosen as 0.17–0.25 (4–6 months). We obtained two main peaks in the MTM spectrum that are located at 4.74 and 5.17 months, respectively.

Figure 13(b) represents the evolution of Rieger-type periods. Periods of length from 4.5 months to 5.5 months were present from ~ 1977 to ~ 1979 that was the ascending phase of the Solar Cycle 21. On the other hand, a big contour of varying length between 4 months and 6 months was prominent from 1983 to 1987 (during the descending phase including minima of Cycle 21); from about 1993 to 1995 (descending phase of Cycle 22); another contour of varying width from 2003 to 2012 (from the maximum of Cycle 23 to the minimum phase of Cycle 24). We have also detected a statistically significant periodicity ($> 95\%$ confidence level) of about 4.5 months during 2016 that was the descending phase of Cycle 24. Rieger-type periods were also prominent in the corresponding MTM plots (Figure 13(a)).

4. Discussions and Conclusions

In this work, we have studied the long-term evolution and different properties of the sunspot penumbra–umbra area ratio using the Debrecen Photoheliographic Data (DPD) sunspot catalog for Cycles 21–24. The main findings of our investigations are summarized below:

- i) We have found that the penumbra to umbra area ratio (q) value starts at ~ 6.4 for small total sunspot areas ($< 100 \mu\text{Hem}$). Then it shows a local minimum of ~ 5.5 in the range of $\sim 100 \mu\text{Hem}$. It maintains a value ~ 6 for the sunspot -area range from $800 \mu\text{Hem}$ to about $3500 \mu\text{Hem}$. However, for very large sunspots with areas $\geq 4500 \mu\text{Hem}$, its value varies from 5.5 to 8.7. In the case of group sunspot-area data, the ratio (q) started from 5.5 and showed some rising nature. The ratio exhibited two strong peaks within the zone $600 \mu\text{Hem}$ to $700 \mu\text{Hem}$. For very large sunspot groups ($\geq 3000 \mu\text{Hem}$), its value varies between 5 and 9.5. We have found that the average value considering all sunspot groups is ~ 6.761 and when the group sunspot-area data $\leq 2000 \mu\text{Hem}$, the mean value of this ratio is ~ 6.735 . These results are partially in agreement with the previous results of Hathaway (2013) and Jha, Mandal, and Banerjee (2019) that the ratio rises from 5.5 to 6 as the sunspot size increases from $100 \mu\text{Hem}$ to $2000 \mu\text{Hem}$.
- ii) We found that this ratio does not depend on the latitude of the sunspot groups in the opposite hemispheres. We did not find any particular trend of variation of this ratio with the change of latitude considering the whole solar disk as well as in the northern and southern hemispheres separately. Further, we have found that this ratio does not exhibit any significant variation or any kind of trend during different phases of the solar cycles as well as cycle strength for the sunspot cycles under study.
- iii) Our histogram plots indicate that the maximum value of the penumbra–umbra ratio changes from cycle to cycle. However, the maxima are confined within the ratio values 4 to 8. Our analysis also showed that both small ($< 100 \mu\text{Hem}$) and large ($\geq 100 \mu\text{Hem}$) sunspot groups follow the trend of solar cycles.
- iv) The power-spectrum analysis methods identified a number of intermediate-term periodicities (> 2 months and ≤ 11 years), including the well-known Rieger and Rieger group quasi-biennial oscillations (QBOs) as well as other midterm periods in the monthly average value of the penumbra–umbra area ratio time series. We have carried out a detailed investigation into the spatiotemporal evolution of Rieger-type periods for the range of 130–190 days by using a wavelet technique and found that modulation and appearance of these types of periods are different in the different cycles. We concluded that the penumbra to umbra area ratio data has a prominent 10–11-year cyclic variations (solar-cycle length).

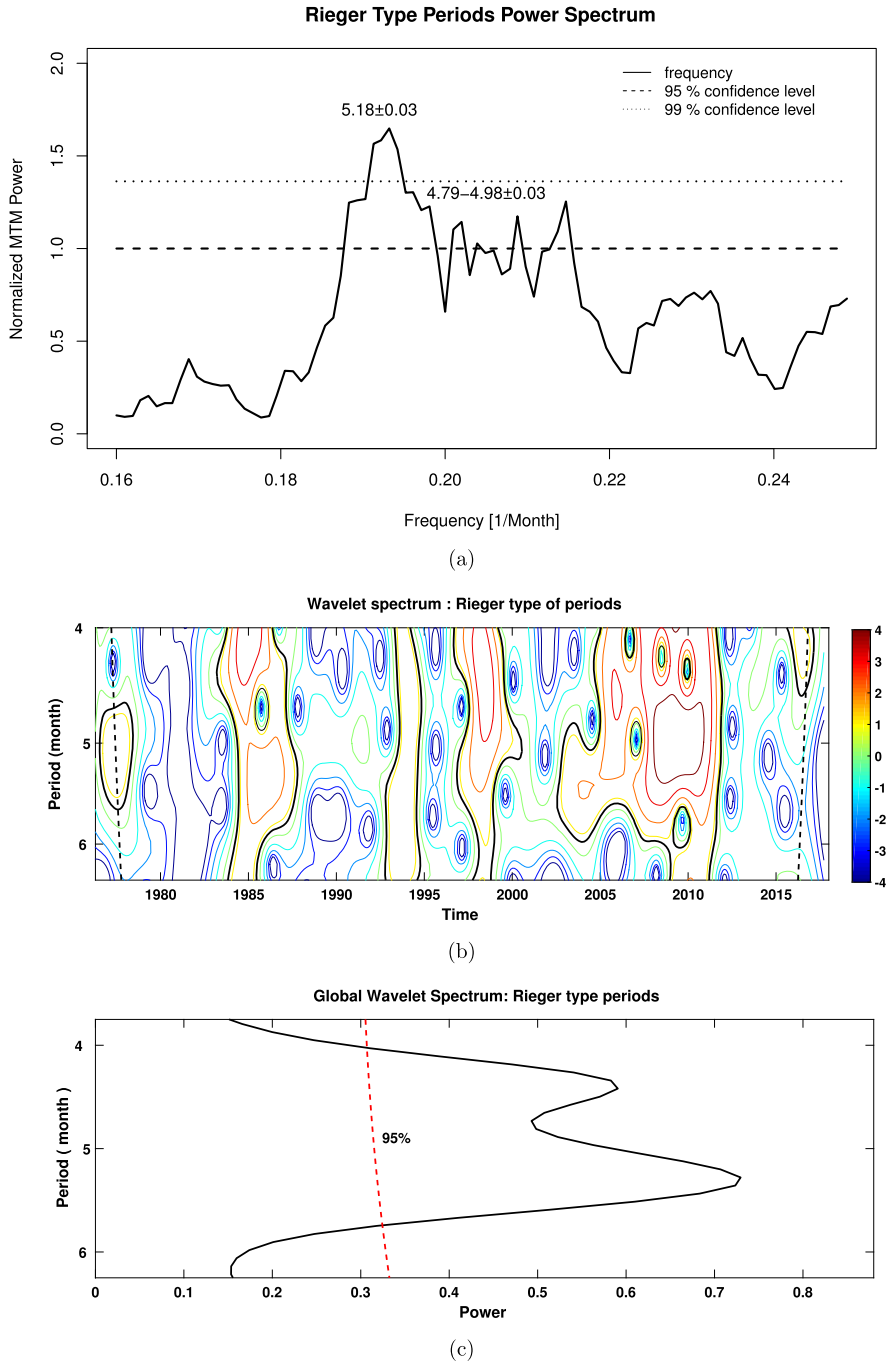


Figure 13 Panel (a) MTM analysis of Rieger-type periods. Panels (b) and (c) exhibit the global and local power spectra of the monthly mean penumbra–umbra ratio data series for the range 4–6 months. The numbers on top mark the detected periods and their possible errors in units of months. The 95% confidence level in GWPS is indicated by the red dotted line.

In this study, we have considered all types of sunspots from smaller ones to larger ones, as published in the DPD catalog. We have found that after some initial variations from ~ 5.5 to ~ 8 , the penumbra–umbra area ratio (q) maintains an average value ~ 6 , as the daily total sunspot area increases from $900 \mu\text{Hem}$ to $7500 \mu\text{Hem}$. However, we have noted that there are two local maxima of q_{avg} within sunspot areas 200 to $500 \mu\text{Hem}$, which requires more investigations for any convincing explanation. In the case of group-sunspot area data, we noted that the ratio showed strong two peaks within $600 \mu\text{Hem}$ to $700 \mu\text{Hem}$. In this region, we have detected several spots with small umbra areas. We have established that the average ratio of the penumbral-to-umbral area considering daily total sunspot area is ~ 6.27 and for the data of group-sunspot area is ~ 6.76 . Hathaway (2013) noted that this penumbra–umbra area ratio increases from 5 to 6 when the sunspot-group area increases from $100 \mu\text{Hem}$ to $2000 \mu\text{Hem}$ using the data from the Royal Greenwich Observatory (RGO) for the time period 1874–1976. A similar result was also obtained by Jha, Mandal, and Banerjee (2019) with the long-term Kodaikanal white-light sunspot area measurement time series. Also, similar results were obtained by Bludova, Obridko, and Badalyan (2014). On the other hand, Takalo (2023) investigated Debrecen sunspot groups and indicated that the average q -value was ~ 5.74 . Hou et al. (2022) used Yunnan Observatories data for the time period from 1957 to 2021, and reported that the ratio of penumbra to umbra area was 6.63 ± 0.98 . The majority of sunspot groups belong to $\leq 2000 \mu\text{Hem}$ and we have found that the average value of this ratio is 6.036 ± 0.044 considering daily sunspot area up to this size, which is very close to the previous report of Hathaway (2013). However, the difference between our result and that of Hathaway (2013) and Jha, Mandal, and Banerjee (2019) probably arises from using different observational data, where the instrument design, measurement method, and calibration processes are different. The umbral area as well as the whole sunspot area measured by Kodaikanal Observatory have differences from those of Debrecen Heliophysical Observatory (see plot 3 of Jha, Mandal, and Banerjee, 2019). Takalo (2023) indicated that the DPD dataset shows the smallest umbral areas, mainly for large sunspots that is different from the data of RGO and Kodaikanal. Javaraiah (2016) also noted that there exists a difference in size and number of different kinds of sunspot groups between the combined Greenwich and SOON data and Debrecen Heliophysical Observatory data between 1974–2015. It was also reported by Jha, Mandal, and Banerjee (2019) that, for the sunspots $< 100 \mu\text{Hem}$, q -values for Kodaikanal data fluctuate between 4 to 5 all the time, and for sunspots $\geq 100 \mu\text{Hem}$ between 5 to 6, while for the other two datasets (RGO and Debrecen) the variation is much larger. Takalo (2023) reported the presence of the Gnevyshev gap (GG) in its temporal evolution of the q -values in the Debrecen dataset. However, for the RGO and Kodaikanal datasets it was shown that the GG region occurred a few months later than the GG in the Debrecen data for Solar Cycles 21–24. We conjecture that these are the main reasons for the different results. Physically, the high value of q indicates that larger sunspots tend to have a larger penumbra. Our analysis supports the findings of Tandberg-Hanssen (1956) and Antalová (1971) that penumbra sizes are larger in large sunspot groups.

We have studied the variations of q in different latitude bands and investigated the nature of this variation considering the opposite hemispheres. We have noted that q does not depend on the latitude of any spot in the northern or in the southern hemisphere, respectively. Moreover, we have found that the nature of the variation of q in the same latitude belt is different in the two hemispheres. This indicates that the dynamic properties and/or the formation of penumbra and umbra are likely different in the northern and southern hemispheres, respectively. The magnetic flux is generated by the dynamo mechanism, which is a global process. In order for the 11-year cycle to persist over many years, the dynamo process must be synchronized between the hemispheres. However, the spots and their structure

are formed from the generated flow directly below the photosphere in the convection zone. The exact mechanism for converting the generated mean flow into spots is still unknown (see, for example, Brandenburg, Kleeorin, and Rogachevskii, 2010), but it is definitely local and therefore not synchronized in the two hemispheres. Hence, there exists north–south asymmetry of the evolution of q in different latitude bands. This result is consistent with the earlier findings of Hathaway (2013) and Takalo (2023) that the q -value does not show variation as a function of latitude.

We have also found that the value of q is different in the different solar cycles under study. In two odd cycles (Cycles 21 and 23), this ratio falls from the starting value and then showed a sudden rise within 500 μ Hem. Above sunspot areas of 500 μ Hem, the ratio gradually comes to a steady value ~ 6 . During Cycle 21 and for large sunspot areas ($> 3000 \mu$ Hem), the q value scatters from 4.5 to 7.5. For the even-numbered Cycles 22 and 24, we have found that after the initial fall and rise in the low sunspot areas ($\leq 200 \mu$ Hem), q showed a tendency to increase and this behavior was maintained for large sunspot areas too. The increase of q with sunspot area for even Cycles 22 and 24 is consistent with previous investigations considering all sunspot groups (Tandberg-Hanssen, 1956; Antalová, 1971). However, more investigations are required to shed light on the dependence of q on the sunspot-cycle strength and odd–even differences.

To study the dependence of q on solar-cycle phases, we have split Cycles 21 to 24 into different phases and determined q in each of these phases separately. In the case of rising and declining phases, q shows a tendency to increase with sunspot area, whereas the ratio maintains a nearly steady value (~ 6) during the maximum phase of the cycles. The ratio q depends on the size of the sunspot/sunspot groups and for larger spots with small umbral area the ratio increases and vice versa. Therefore, the variation of q in different solar cycles as well as different phases of any cycle depends on the size of the spots present in those phases. Kilcik et al. (2011) considered the sunspot-group data of different observatories and indicated that, in general, large sunspot groups peaked about two years later than the small ones in the solar cycle. Javaraiah (2016) utilized the sunspot-group data from the combined Greenwich and SOON Observatories as well as the DPD catalog and reported that in many cycles the positions of the peaks of the small and large sunspot groups are different, and they also deviate considerably from the corresponding peak positions of sunspot number. These factors are probably reflected in Figure 8, where we have seen that the magnitude of q varies from cycle to cycle and the peak value of q has some mismatch in time with the peak value of the sunspot number. In future, we aim to study this factor in more detail. During Cycles 21 and 23, q exhibits a large scatter in the minimum phase and this nature is absent in Cycle 22. All these indicate that q differs in different phases as well as different solar cycles and does not possess any particular trend.

We have segregated the spots according to their sizes and studied their dynamical behavior for each cycle under study. Our analysis shows that small sunspot groups ($< 100 \mu$ Hem), the penumbra–umbra area ratio follows the nature of solar -cycle variations. This result is in close agreement with the recent detection of Carrasco et al. (2018) who analyzed Coimbra Astronomical Observatory sunspot data for the time period 1929–1941. However, our study also reveals, for spot groups with areas $> 100 \mu$ Hem, that this ratio is noisy and does not exhibit any tendency to follow the solar cycles. This result is in accordance with the observations made by Jha, Mandal, and Banerjee (2019) with the Kodaikanal dataset. In both types of spots we have detected some decrease in q value that may be related with the GG as indicated by Takalo (2023). We have further pointed out that 13-month moving average values of q exhibit an 11-year periodic nature like other sunspot indices.

Next, we have used the multitaper method (MTM) and a complex Morlet-wavelet analysis tool to detect the intermediate-term periodicities (> 2 months to ≤ 11 years) in the

penumbra–umbra ratio dataset considering that both the period and amplitude of different oscillations may vary from cycle to cycle (Hathaway, 2015; Chowdhury et al., 2022). The employed power-spectral analysis methods identified the presence of Rieger-type periods, quasibiennial oscillations (QBOs), as well as ~ 11 year sunspot cycle periods. Further, we have explored the evolutions of Rieger-type periods in different cycles under study with a wavelet technique. Previously, the above-mentioned periods and their solar-cycle variations were reported in different solar and helioseismic indices (Oliver, Carbonell, and Ballester, 1992; Krivova and Solanki, 2002; Chowdhury, Jain, and Awasthi, 2013; Vecchio et al., 2012; Broomhall and Nakariakov, 2015; Kiss and Erdélyi, 2018; Kilcik et al., 2020; Xiang, Ning, and Li, 2020; Zhang et al., 2022; Korsós et al., 2023, and references therein).

These are key findings here and so far to the best of our knowledge it is the first report of detection of periodic/quasiperiodic behavior of penumbra–umbra area ratio data.

Till now there exists no physics-based model for a clear explanation about different features of these intermediate-term periods. Bai and Sturrock (1993) and Bai (2003) suggested that the presence of a 40° -tilted obliquely rotating structure having a rotation period of 25.5 day produces Rieger-type periods for an offaxis rotating solar core distorted by a strong toroidal magnetic field (see Dicke, 1979) but such a type of structure has not been detected yet. The ~ 2 -year QBOs are possibly connected with the dynamics of the solar inner layers (Kiss and Erdélyi, 2018; Inceoglu et al., 2019; Hazra, Brun, and Nandy, 2020). The prominent ~ 11 -year periodicity in penumbra–umbra area ratio data is similar to that of the Schwabe cycle period of sunspot activities and is probably associated with the variations of the large-scale magnetic field due to the global nonlinear dynamo mechanism occurring inside the Sun (see Hazra and Nandy, 2016, 2019; Charbonneau, 2020, for details). Ballester, Oliver, and Carbonell (2002, 2004) indicated that there is an association with the periodic emergence of magnetic flux from the interior to the solar-surface complex active regions and the periodic behavior of Rieger-type periods. On the other hand, Zaqarashvili et al. (2010a) argued that Rieger-type periods are produced when the field strength is $\leq 10^4$ G in the upper overshoot layer of the tachocline. Magnetic-field strengths $\geq 10^5$ G near the lower layers of the tachocline create the periods of ~ 2 years (Zaqarashvili et al., 2010b). Several researchers indicated that the different observed quasiperiodicities are governed by the dynamics of magnetic Rossby and mixed Rossby–Poincaré hydrodynamic-type waves present in the solar atmosphere (Lou, 2000; Ulrich, 2001; Sturrock et al., 2013; Gurgenshvili et al., 2016, 2017; Dikpati et al., 2018, etc.). These types of waves have been detected in the deep solar interior (Löptien et al., 2018; Liang et al., 2019; Proxauf et al., 2020; Hathaway and Upton, 2021; Korsós et al., 2023, etc.) as well as in the bright points of corona (McIntosh et al., 2017) from the data of Solar Terrestrial Relations Observatory (STEREO) and Solar Dynamics Observatory (SDO) spacecraft. Further, Lanza et al. (2009) reported the existence of such magnetic Rossby waves in the atmosphere of many sun-like stars. Some researchers suggested that different solar midterm periodicities could be explained considering suitable spherical harmonics of magneto-Rossby types of waves (Dimitropoulou, Moussas, and Strintzi, 2008; Zaqarashvili, 2018; Chowdhury et al., 2019, 2022; Gachechiladze et al., 2019; Bilenko, 2020). For more details about the relation between different midterm periods and Rossby-type waves see Ruždjak et al. (2023). Recently, Zaqarashvili et al. (2021) have discussed the connection between the different kinds of solar periodicities with magneto-Rossby waves generated in the solar-interior dynamo layer. However, more investigations about tachocline instability properties due to magnetohydrodynamic (MHD) waves are required to determine the exact reason behind different quasiperiodicities detected in solar datasets.

Periodicities of three to seven years are sometimes referred to as intermediate or medium-term quasiperiodicities (e.g., Lou et al., 2003). The so-called quasibiennial oscillations, or

QBOs, are the most well-known midterm oscillations (MTOs) (see, for example, the comprehensive review by Bazilevskaya et al., 2014, and references therein). Six-year oscillations have also been described as a midterm periodicity (Prabhakaran Nayar et al., 2002; Ravindra et al., 2022). In a Sun as a star observation, Rivin and Obridko (1992) found that these changes could be seen even in the Sun's whole magnetic field. Sokoloff et al. (2020) suggested the name Quasi-Sexennial Oscillations (QSO) for these variations. The two parts of the MTO (QBO and QSO) have different characteristics and may have come from different origins. Sokoloff et al. (2020) concluded that both the sunspot-number record and proxies for the Sun's overall magnetic field, such as the evolution of the solar axial dipole, show evidence of QSO. Dynamo models demonstrate that these QSO are caused by the dynamo cycle's nonlinear, anharmonic shape. Long-term variations in QSO are the result of inter-scale dynamics brought on by sunspot formation at the solar surface and long-term dynamo variations.

It should be noted that the parameter q is a very fine indicator of the structure of an active region. The fact is that the global dynamo generates only the general flux of the magnetic field, and as a result, determines the 11-year cycle. However, the direct formation of sunspots and active regions in general takes place directly near the photosphere, probably in the leptocline. An analysis of the emergence of an active region was studied in the works of Getling, Ishikawa, and Buchnev (2016), Getling and Buchnev (2019), Zagainova et al. (2022). The early stage of AR formation includes the floating up of a new magnetic flux in the form of a chaotic mixture of magnetic elements of different polarity (Smirnova et al., 2013). At the same time, the penumbra is formed as a result of channelized convection at the periphery of the magnetic-flux tube (Kosovichev, 2009, 2012). This is a rather individual process, so the dependence of q index on the latitude and phase of the cycle ceases to be noticeable.

On the other hand, the processes of ascent, the evolution of the active region, and the development of the penumbra are apparently clearly balanced. During the evolution of the active region, the magnetic field and the total area change by tens and even hundreds of times, and the q index changes by no more than 20–40%. On the Sun, we have never observed large spots consisting entirely of umbra or penumbra. Whether this is a specific feature of the sunspot-formation process on the Sun, we do not yet know.

In the near future, our aim is to continue this investigation by using the penumbra–umbra area time series from other observatories including space-borne satellites like the Michelson Doppler Imager (MDI) (Scherrer et al., 1995) continuum images from Solar and Helioseismic Observatory (SOHO); Helioseismic and Magnetic Imager (HMI) (Scherrer et al., 2012) on board Solar Dynamics Observatory (SDO) (Schou et al., 2012, etc). This will be helpful for us to explore images of higher spatial resolution with more accuracy. These findings may shed some light onto our understanding formation of penumbra, dynamo models of sunspot magnetic-field activities, decay of sunspots, and changes in the solar irradiance in the recent past solar cycles.

According to the established relationships, the relative umbral area and the relative number of small groups are crucial elements in determining the secular variation of solar activity. They could explain variations in the mean magnetic field in active regions, the complexity of a group based on magnetic classification, the flare activity of a sunspot group, and its geophysical implications, in particular. The parameter q is hypothesized to describe the leptocline's time-varying relative contribution from the interior and subsurface dynamo mechanisms.

Acknowledgments We thank the anonymous reviewer for very useful comments that helped to greatly improve the manuscript. The authors acknowledge the work of all the people who contribute to and maintain

the DPD Sunspot database. P. Chowdhury thanks D. Hathaway, D. Banerjee, Sudip Mandal, and Bibhuti Jha for scientific discussions.

Author contributions All analysis made by Partha Chowdhury, Ankit Saha and Ali Kilcik, and the draft manuscript has been prepared by them. J.P. Rozelot, V. Obridko and R. Erdélyi made great contributions especially on the final stage of the manuscript. Also they contributed on the physical explanation of the obtained results. All authors read the manuscript carefully and improved the language.

Funding Open access funding provided by the Scientific and Technological Research Council of Türkiye (TÜBİTAK). R. Erdélyi is also grateful to the Science and Technology Facilities Council (STFC, grant Nos. ST/M000826/1 and NKFIH (OTKA, grant No. K142987) Hungary) for the support received. R.E. also acknowledges the support received by the CAS Presidents International Fellowship Initiative grant No.2019VMA052, the Royal Society. The work of VO was supported by RNF grant No. 21–72–20067.

Declarations

Competing interests The authors declare no competing interests.

Open Access This article is licensed under a Creative Commons Attribution 4.0 International License, which permits use, sharing, adaptation, distribution and reproduction in any medium or format, as long as you give appropriate credit to the original author(s) and the source, provide a link to the Creative Commons licence, and indicate if changes were made. The images or other third party material in this article are included in the article's Creative Commons licence, unless indicated otherwise in a credit line to the material. If material is not included in the article's Creative Commons licence and your intended use is not permitted by statutory regulation or exceeds the permitted use, you will need to obtain permission directly from the copyright holder. To view a copy of this licence, visit <http://creativecommons.org/licenses/by/4.0/>.

References

- Antalová, A.: 1971, The ratio of penumbral and umbral areas of sun-spots in the 11-year solar activity cycle. *Bull. Astron. Inst. Czechoslov.* **22**, 352.
- Antalová, A.: 1991, The relation of the sunspot magnetic field and penumbra-umbra radius ratio. *Bull. Astron. Inst. Czechoslov.* **42**, 316.
- Bai, T.: 2003, Periodicities in solar flare occurrence: analysis of cycles 19–23. *Astrophys. J.* **591**, 406. DOI.
- Bai, T., Cliver, E.W.: 1990, A 154 day periodicity in the occurrence rate of proton flares. *Astrophys. J.* **363**, 299. DOI.
- Bai, T., Sturrock, P.A.: 1993, Evidence for a fundamental period of the Sun and its relation to the 154 day complex of periodicities. *Astrophys. J.* **409**, 476. DOI.
- Ballester, J.L., Oliver, R., Carbonell, M.: 2002, The near 160 day periodicity in the photospheric magnetic flux. *Astrophys. J.* **566**, 505.
- Ballester, J.L., Oliver, R., Carbonell, M.: 2004, Return of the near 160 day periodicity in the photospheric magnetic flux during solar cycle 23. *Astrophys. J. Lett.* **615**, L173. DOI.
- Baranyi, T., Györi, L., Ludmány, A.: 2016, On-line tools for solar data compiled at the debrecen observatory and their extensions with the greenwich sunspot data. *Solar Phys.* **291**, 3081. DOI.
- Bazilevskaya, G., Broomhall, A.M., Elsworth, Y., Nakariakov, V.M.: 2014, A combined analysis of the observational aspects of the quasi-biennial oscillation in solar magnetic activity. *Space Sci. Rev.* **186**, 359. DOI.
- Bazilevskaya, G.A., Kalinin, M.S., Krainev, M.B., Makhmutov, V.S., Svirzhevskaya, A.K., Svirzhevsky, N.S., Stozhkov, Y.I.: 2022, On the reproduction of the solar activity variations in the range 2–40 months in the interplanetary medium. *Sov. Phys. JETP* **134**, 479. DOI.
- Bilenko, I.A.: 2020, Manifestation of Rossby waves in the global magnetic field of the Sun during cycles 21–24. *Astrophys. J. Lett.* **897**, L24. DOI.
- Bludova, N.G., Obridko, V.N., Badalyan, N.: 2014, The relative umbral area in spot groups as an index of cyclic variation of solar activity. *Solar Phys.* **289**, 1013.
- Bogart, R.S., Bai, T.: 1985, Confirmation of a 152 day periodicity in the occurrence of solar flares inferred from microwave data. *Astrophys. J. Lett.* **299**, L51. DOI.
- Borrero, J.M., Ichimoto, K.: 2011, Magnetic structure of sunspots. *Living Rev. Solar Phys.* **8**, 4. DOI.

- Brandenburg, A., Klecorin, N., Rogachevskii, I.: 2010, Large-scale magnetic flux concentrations from turbulent stresses. *Astron. Nachr.* **331**, 5. DOI. ADS.
- Brandt, P.N., Schmidt, W., Steinegger, M.: 1990, On the umbra / penumbra area ratio of sunspots. *Solar Phys.* **129**, 191. DOI.
- Bray, R.J., Loughhead, R.E.: 1964 *Sunspots. The International Astrophysics Series*, Chapman & Hall, London.
- Broomhall, A.M., Nakariakov, V.M.: 2015, A comparison between global proxies of the Sun's magnetic activity cycle: inferences from helioseismology. *Solar Phys.* **290**, 3095. DOI.
- Carbonell, M., Ballester, J.L.: 1992, The periodic behaviour of solar activity – the near 155-day periodicity in sunspot areas. *Astron. Astrophys.* **255**, 350.
- Carrasco, V.M.S., Vaquero, J.M., Trigo, R.M., Gallego, M.C.: 2018, A curious history of sunspot penumbrae: an update. *Solar Phys.* **293**, 104. DOI.
- Charbonneau, P.: 2020, Dynamo models of the solar cycle. *Living Rev. Solar Phys.* **17**, 4. DOI.
- Chowdhury, P., Jain, R., Awasthi, A.K.: 2013, Periodicities in the X-ray emission from the solar corona. *Astrophys. J.* **778**, 9.
- Chowdhury, P., Khan, M., Ray, P.C.: 2009, Intermediate-term periodicities in sunspot areas during solar cycles 22 and 23. *Mon. Not. Roy. Astron. Soc.* **392**, 1159.
- Chowdhury, P., Gokhale, M.H., Singh, J., Moon, Y.J.: 2016, Mid-term quasi-periodicities in the CaII-K plage index of the Sun and their implications. *Astrophys. Space Sci.* **361**, 54. DOI.
- Chowdhury, P., Kilcik, A., Yurchyshyn, V., Obridko, V.N., Rozelot, J.P.: 2019, Analysis of the hemispheric sunspot number time series for the solar cycles 18 to 24. *Solar Phys.* **294**, 142. DOI.
- Chowdhury, P., Belur, R., Bertello, L., Pevtsov, A.A.: 2022, Analysis of solar hemispheric chromosphere properties using the kodaikanal observatory Ca-K index. *Astrophys. J.* **925**, 81. DOI.
- de Paula, V., Curto, J.J., Oliver, R.: 2022, The cyclic behaviour in the N-S asymmetry of sunspots and solar plages for the period 1910 to 1937 using data from Ebro catalogues. *Mon. Not. Roy. Astron. Soc.* **512**, 5726. DOI.
- Di Matteo, S., Villante, U.: 2017, The identification of solar wind waves at discrete frequencies and the role of the spectral analysis techniques. *J. Geophys. Res.* **122**, 4905. DOI.
- Dicke, R.H.: 1979, The clock inside the Sun. *New Sci.* **83**, 12. ADS.
- Dikpati, M., McIntosh, S.W., Bothun, G., Cally, P.S., Ghosh, S.S., Gilman, P.A., Umurhan, O.M.: 2018, Role of interaction between magnetic Rossby waves and tachocline differential rotation in producing solar seasons. *Astrophys. J.* **853**, 144. DOI.
- Dimitropoulou, M., Moussas, X., Strintzi, D.: 2008, Enhanced Rieger-type periodicities' detection in X-ray solar flares and statistical validation of Rossby waves' existence. *Mon. Not. Roy. Astron. Soc.* **386**, 2278. DOI.
- Dobrica, V., Demetrescu, C., Mares, I., Mares, C.: 2018, Long-term evolution of the lower Danube discharge and corresponding climate variations: solar signature imprint. *Theor. Appl. Climatol.* **133**, 985. DOI.
- Gachechiladze, T., Zaqarashvili, T.V., Gurgenchashvili, E., Ramishvili, G., Carbonell, M., Oliver, R., Ballester, J.L.: 2019, Magneto-Rossby waves in the solar tachocline and the annual variations in solar activity. *Astrophys. J.* **874**, 162. DOI.
- Gao, P.-X., Li, K.-J., Li, F.-Y.: 2017, Possible explanation of the different temporal behaviors of various classes of sunspot groups. *Solar Phys.* **292**, 124. DOI.
- Getling, A.V., Buchnev, A.A.: 2019, The origin and early evolution of a bipolar magnetic region in the solar photosphere. *Astrophys. J.* **871**, 224. DOI.
- Getling, A.V., Ishikawa, R., Buchnev, A.A.: 2016, Development of active regions: flows, magnetic-field patterns and bordering effect. *Solar Phys.* **291**, 371.
- Ghil, M., Allen, M.R., Dettinger, M.D., Ide, K., Kondrashov, D., Mann, M.E., Robertson, A.W., Saunders, A., Tian, Y., Varadi, F., Yiou, P.: 2002, Advanced spectral methods for climatic time series. *Rev. Geophys.* **40**, 1003. DOI.
- Gnevyshev, M.N.: 1967, On the 11-years cycle of solar activity. *Solar Phys.* **1**, 107. DOI.
- Grinsted, A., Moore, J.C., Jevrejeva, S.: 2004, Application of the cross wavelet transform and wavelet coherence to geophysical time series. *Nonlinear Process. Geophys.* **11**, 561. DOI. ADS.
- Gurgenchashvili, E., Zaqarashvili, T.V., Kukhianidze, V., Oliver, R., Ballester, J.L., Ramishvili, G., Shergelashvili, B., Hanslmeier, A., Poedts, S.: 2016, Rieger-type periodicity during solar cycles 14-24: estimation of dynamo magnetic field strength in the solar interior. *Astrophys. J.* **826**, 55. DOI.
- Gurgenchashvili, E., Zaqarashvili, T.V., Kukhianidze, V., Oliver, R., Ballester, J.L., Dikpati, M., McIntosh, S.W.: 2017, North-south asymmetry in rieger-type periodicity during solar cycles 19-23. *Astrophys. J.* **845**, 137. DOI.
- Györi, L.: 1998, Automation of area measurement of sunspots. *Solar Phys.* **180**, 109. DOI.
- Györi, L.: 2005, Automated determination of the alignment of solar images. *Hvar Obs. Bull.* **29**, 299.

- Györi, L., Baranyi, T., Ludmány, A.: 2011, Photospheric data programs at the debrecen observatory. In: *The Physics of Sun and Star Spots, Proceedings of the International Astronomical Union, IAU Symposium 273*, 403.
- Györi, L., Ludmány, A., Baranyi, T.: 2017, Comparative analysis of debrecen sunspot catalogues. *Mon. Not. Roy. Astron. Soc.* **465**, 1259. DOI.
- Hathaway, D.H.: 2013, A curious history of sunspot penumbrae. *Solar Phys.* **286**, 347. DOI.
- Hathaway, D.H.: 2015, The solar cycle. *Living Rev. Solar Phys.* **12**, 4. DOI.
- Hathaway, D.H., Upton, L.A.: 2021, Hydrodynamic properties of the Sun's giant cellular flows. *Astrophys. J.* **908**, 160. DOI. ADS.
- Hathaway, D.H., Wilson, R.M., Campbell, A.: 2007, Curious behavior of sunspot umbrae in the first half of the 20th century. *Bull. Am. Astron. Soc.* **39**, 209.
- Hazra, S., Brun, A.S., Nandy, D.: 2020, Does the mean-field α effect have any impact on the memory of the solar cycle? *Astron. Astrophys.* **642**, A51. DOI.
- Hazra, S., Nandy, D.: 2016, A proposed paradigm for solar cycle dynamics mediated via turbulent pumping of magnetic flux in babcock-leighton-type solar dynamos. *Astrophys. J.* **832**, 9. DOI.
- Hazra, S., Nandy, D.: 2019, The origin of parity changes in the solar cycle. *Mon. Not. Roy. Astron. Soc.* **489**, 4329. DOI.
- Hou, J.-W., Zeng, S.-G., Zheng, S., Luo, X.-Y., Deng, L.-H., Li, Y.-Y., Chen, Y.-Q., Lin, G.-H., Feng, Y.-L., Tao, J.-P.: 2022, Chinese sunspot drawings and their digitization-(VII) sunspot penumbra to umbra area ratio using the hand-drawing records from Yunnan observatories. *Res. Astron. Astrophys.* **22**, 095012. DOI. ADS.
- Inceoglu, F., Simonello, R., Arlt, R., Rempel, M.: 2019, Constraining non-linear dynamo models using quasi-biennial oscillations from sunspot area data. *Astron. Astrophys.* **625**, A117. DOI.
- Javaraiah, J.: 2016, North-south asymmetry in small and large sunspot group activity and violation of even-odd solar cycle rule. *Astrophys. Space Sci.* **361**, 208. DOI. ADS.
- Jensen, E., Nordø, J., Ringnes, T.S.: 1955, Variations in the structure of sunspots in relation to the sunspot cycle. *Astrophys. Nor.* **5**, 167.
- Jha, B.K., Mandal, S., Banerjee, D.: 2019, Study of sunspot penumbra to umbra area ratio using kodaikanal white-light digitised data. *Solar Phys.* **294**, 72. DOI.
- Jurčák, J., Bello González, N., Schlichenmaier, R., Rezaei, R.: 2017, A distinct magnetic property of the inner penumbral boundary. II. Formation of a penumbra at the expense of a pore. *Astron. Astrophys.* **597**, A60. DOI.
- Kilcik, A., Yurchyshyn, V.B., Abramenko, V., Goode, P.R., Ozguc, A., Rozelot, J.P., Cao, W.: 2011, Time distributions of large and small sunspot groups over four solar cycles. *Astrophys. J.* **731**, 30. DOI.
- Kilcik, A., Yurchyshyn, V., Donmez, B., Obridko, V.N., Ozguc, A., Rozelot, J.P.: 2018, Temporal and periodic variations of sunspot counts in flaring and non-flaring active regions. *Solar Phys.* **293**, 63. DOI.
- Kilcik, A., Chowdhury, P., Sarp, V., Yurchyshyn, V., Donmez, B., Rozelot, J.-P., Ozguc, A.: 2020, Temporal and periodic variation of the MCMESI for the last two solar cycles; comparison with the number of different class X-ray solar flares. *Solar Phys.* **295**, 159. DOI.
- Kiss, T.S., Erdélyi, R.: 2018, On quasi-biennial oscillations in chromospheric macrospicules and their potential relation to the global solar magnetic field. *Astrophys. J.* **857**, 113. DOI.
- Knaack, R., Stenflo, J.O., Berdyugina, S.V.: 2005, Evolution and rotation of large-scale photospheric magnetic fields of the Sun during cycles 21-23. Periodicities, north-south asymmetries and R-mode signatures. *Astron. Astrophys.* **438**, 1067. DOI.
- Korsós, M.B., Dikpati, M., Erdélyi, R., Liu, J., Zuccarello, F.: 2023, On the connection between rieger-type and magneto-Rossby waves driving the frequency of the large solar eruptions during solar cycles 19-25. *Astrophys. J.* **944**, 180. DOI. ADS.
- Kosovichev, A.G.: 2009, Photospheric and subphotospheric dynamics of emerging magnetic flux. *Space Sci. Rev.* **144**, 175. DOI.
- Kosovichev, A.G.: 2012, Local helioseismology of sunspots: current status and perspectives. *Solar Phys.* **279**, 323. DOI.
- Kosovichev, A.G., Rozelot, J.P.: 2018, Solar cycle variations of rotation and asphericity in the near-surface shear layer. *J. Atmos. Solar-Terr. Phys.* **176**, 21. DOI.
- Kotzé, P.B.: 2021, Rieger periodicity behaviour in solar mg II 280 nm spectral emission. *Solar Phys.* **296**, 44. DOI.
- Krivova, N.A., Solanki, S.K.: 2002, The 1.3-year and 156-day periodicities in sunspot data: wavelet analysis suggests a common origin. *Astron. Astrophys.* **394**, 701. DOI.
- Lanza, A.F., Pagano, I., Leto, G., Messina, S., Aigrain, S., Alonso, R., Auvergne, M., Baglin, A., Barge, P., Bonomo, A.S., Boumier, P., Collier Cameron, A., Comparato, M., Cutispoto, G., de Medeiros, J.R., Foing, B., Kaiser, A., Moutou, C., Parihar, P.S., Silva-Valio, A., Weiss, W.W.: 2009, Magnetic activity in the photosphere of CoRoT-Exo-2a. Active longitudes and short-term spot cycle in a young sun-like star. *Astron. Astrophys.* **493**, 193. DOI.

- Lean, J.: 1990, Evolution of the 155 day periodicity in sunspot areas during solar cycles 12 to 21. *Astrophys. J.* **363**, 718. DOI.
- Liang, Z.-C., Gizon, L., Birch, A.C., Duvall, T.L.: 2019, Time-distance helioseismology of solar Rossby waves. *Astron. Astrophys.* **626**, A3. DOI.
- Löptien, B., Gizon, L., Birch, A.C., Schou, J., Proxauf, B., Duvall, T.L., Bogart, R.S., Christensen, U.R.: 2018, Global-scale equatorial Rossby waves as an essential component of solar internal dynamics. *Nat. Astron.* **2**, 568. DOI. ADS.
- Lou, Y.-Q.: 2000, Rossby-type wave-induced periodicities in flare activities and sunspot areas or groups during solar maxima. *Astrophys. J.* **540**, 1102. DOI.
- Lou, Y.Q., Wang, Y.M., Fan, Z., Wang, J.X., Wang, S.: 2003, Periodicities in solar coronal mass ejections. *Mon. Not. Roy. Astron. Soc.* **345**, 809.
- McIntosh, S.W., Cramer, W.J., Pichardo Marcano, M., Leamon, R.J.: 2017, The detection of Rossby-like waves on the Sun. *Nat. Astron.* **1**, 0086. DOI.
- Nicholson, S.B.: 1933, The area of a sun-spot and the intensity of its magnetic field. *Publ. Astron. Soc. Pac.* **45**, 51. DOI.
- Obridko, V.N., Katsova, M.M., Sokoloff, D.D., Shelting, B.D., Livshits, I.M.: 2022, Clarifying physical properties of magnetic fields in sunspots. *Solar Phys.* **297**, 131. DOI. ADS.
- Oliver, R., Ballester, J.L., Baudin, F.: 1998, Emergence of magnetic flux on the Sun as the cause of a 158-day periodicity in sunspot areas. *Nature* **394**, 552. DOI.
- Oliver, R., Carbonell, M., Ballester, J.L.: 1992, Intermediate-term periodicities in solar activity. *Solar Phys.* **137**, 141.
- Ozguc, A., Kilcik, A., Yurchyshyn, V.: 2022, Temporal and periodic variations of the solar flare index during the last four solar cycles and their association with selected geomagnetic-activity parameters. *Solar Phys.* **297**, 112. DOI.
- Ozguc, A., Kilcik, A., Sarp, V., Yesilyaprak, H., Pektas, R.: 2021, Periodic variation of solar flare index for the last solar cycle (cycle 24). *Adv. Astron.* **2021**, 5391091. DOI.
- Park, J.: 1992, Envelope estimation for quasi-periodic geophysical signals in noise: a multitaper approach. In: *Statistics in the Environmental and Earth Sciences*, Arnold, London, 189.
- Percival, D.B., Walden, A.T.: 1993, *Spectral Analysis for Physical Applications*, Cambridge University Press, Cambridge, 978. DOI.
- Prabhakaran Nayar, S.R., Radhika, V.N., Revathy, K., Ramadas, V.: 2002, Wavelet analysis of solar, solar wind and geomagnetic parameters. *Solar Phys.* **208**, 359. DOI.
- Proxauf, B., Gizon, L., Löptien, B., Schou, J., Birch, A.C., Bogart, R.S.: 2020, Exploring the latitude and depth dependence of solar Rossby waves using ring-diagram analysis. *Astron. Astrophys.* **634**, A44. DOI. ADS.
- Ravindra, B., Chowdhury, P., Javaraiah, J.: 2021, Solar-cycle characteristics in kodaikanal sunspot area: North-south asymmetry, phase distribution and gnevyshev gap. *Solar Phys.* **296**, 2. DOI.
- Ravindra, B., Chowdhury, P., Ray, P.C., Pichamani, K.: 2022, Temporal evolutions and quasiperiodic variations present in the sunspot number and group sunspot area data measured at kodaikanal observatory for solar cycles 14-24. *Astrophys. J.* **940**, 43. DOI.
- Rieger, E., Kanbach, G., Reppin, C., Share, G.H., Forrest, D.J., Chupp, E.L.: 1984, A 154-day periodicity in the occurrence of hard solar flares? *Nature* **312**, 623. DOI.
- Rivin, Y.R., Obridko, V.N.: 1992, Frequency composition of long-period magnetic field variations of the sun as a star. *Astron. Zh.* **69**, 1083.
- Ruždjak, D., Brajša, R., Skokić, I., Sudar, D., Hanslmeier, A.: 2023, On the periodicities in solar rotation and activity determined from sunspot-group data and possible connection with Rossby-like waves. *Solar Phys.* **298**, 39. DOI. ADS.
- Scherrer, P.H., Bogart, R.S., Bush, R.I., Hoeksema, J.T., Kosovichev, A.G., Schou, J., Rosenberg, W., Springer, L., Tarbell, T.D., Title, A., Wolfson, C.J., Zayer, I., MDI Engineering Team: 1995, The solar oscillations investigation – Michelson Doppler imager. *Solar Phys.* **162**, 129. DOI.
- Scherrer, P.H., Schou, J., Bush, R.I., Kosovichev, A.G., Bogart, R.S., Hoeksema, J.T., Liu, Y., Duvall, T.L., Zhao, J., Title, A.M., Schrijver, C.J., Tarbell, T.D., Tomczyk, S.: 2012, The Helioseismic and Magnetic Imager (HMI) investigation for the Solar Dynamics Observatory (SDO). *Solar Phys.* **275**, 207. DOI.
- Schou, J., Borrero, J.M., Norton, A.A., Tomczyk, S., Elmore, D., Card, G.L.: 2012, Polarization calibration of the Helioseismic and Magnetic Imager (HMI) onboard the Solar Dynamics Observatory (SDO). *Solar Phys.* **275**, 327. DOI.
- Smirnova, V., Efmov, V.I., Parfinenko, L.D., Riehoakainen, A., Solov'ev, A.A.: 2013, Artifacts of SDO/HMI data and long-period oscillations of sunspots. *Astron. Astrophys.* **554**, A121. DOI.
- Sokoloff, D.D., Shibalova, A.S., Obridko, V.N., Pipin, V.V.: 2020, Shape of solar cycles and mid-term solar activity oscillations. *Mon. Not. Roy. Astron. Soc.* **497**, 4376. DOI.
- Solanki, S.K., Inhester, B., Schüssler, M.: 2006, The solar magnetic field. *Rep. Prog. Phys.* **69**, 563. DOI.

- Sturrock, P.A., Bertello, L., Fischbach, E., Javoresek, D., Jenkins, J.H., Kosovichev, A., Parkhomov, A.G.: 2013, An analysis of apparent R-mode oscillations in solar activity, the solar diameter, the solar neutrino flux, and nuclear decay rates, with implications concerning the Sun's internal structure and rotation, and neutrino processes. *Astropart. Phys.* **42**, 62. DOI.
- Takalo, J.: 2023, Temporal and latitudinal variation in penumbra-umbra ratios of the sunspots: analyses of RGO, kodaikanal and debrecen databases. *Solar Phys.* **298**, 63. DOI. ADS.
- Tandberg-Hanssen, E.: 1955, On the correlation between radio-frequency radiation from the Sun and solar activity. *Astrophys. J.* **121**, 367. DOI.
- Tandberg-Hanssen, E.: 1956, A study of the penumbra-umbra ratio of sunspot pairs. *Astrophys. Nor.* **5**, 207.
- Thomson, D.J.: 1982, Spectrum estimation and harmonic analysis. *Proc. IEEE* **70**, 1055.
- Torrence, C., Compo, G.P.: 1998, A practical guide to wavelet analysis. *Bull. Am. Meteorol. Soc.* **79**, 61.
- Ulrich, R.K.: 2001, Very long lived wave patterns detected in the solar surface velocity signal. *Astrophys. J.* **560**, 466. DOI.
- Vaquero, J.M., Gordillo, A., Gallego, M.C., Sanchez-Bajo, F., Garcia, J.A.: 2005, The umbra-penumbra area ratio of sunspots from the de la Rue data. *Observatory* **125**, 152.
- Vecchio, A., Laurenza, M., Meduri, D., Carbone, V., Storini, M.: 2012, The dynamics of the solar magnetic field: polarity reversals, butterfly diagram, and quasi-biennial oscillations. *Astrophys. J.* **749**, 27. DOI.
- Waldmeier, M.: 1939, Über die Struktur der Sonnenflecken. *Astron. Mitt. (Zür.)* **14**, 439.
- Xiang, N.B., Ning, Z.J., Li, F.Y.: 2020, Temporal evolution of the rotation of the interplanetary magnetic field B_x , B_y , and B_z components. *Astrophys. J.* **896**, 12. DOI.
- Zagainova, Y.S., Fainshtein, V.G., Obridko, V.N., Rudenko, G.V.: 2022, Study of the magnetic properties of sunspot umbrae. *Astron. Rep.* **66**, 116. DOI.
- Zaqarashvili, T.: 2018, Equatorial magnetohydrodynamic shallow water waves in the solar tachocline. *Astrophys. J.* **856**, 32. DOI.
- Zaqarashvili, T.V., Carbonell, M., Oliver, R., Ballester, J.L.: 2010a, Magnetic Rossby waves in the solar tachocline and rieger-type periodicities. *Astrophys. J.* **709**, 749. DOI.
- Zaqarashvili, T.V., Carbonell, M., Oliver, R., Ballester, J.L.: 2010b, Quasi-biennial oscillations in the solar tachocline caused by magnetic Rossby wave instabilities. *Astrophys. J. Lett.* **724**, L95. DOI.
- Zaqarashvili, T.V., Albekioni, M., Ballester, J.L., Bekki, Y., Biancofiore, L., Birch, A.C., Dikpati, M., Gizon, L., Gurgenchashvili, E., Heifetz, E., Lanza, A.F., McIntosh, S.W., Ofman, L., Oliver, R., Proxauf, B., Umurhan, O.M., Yellin-Bergovoy, R.: 2021, Rossby waves in astrophysics. *Space Sci. Rev.* **217**, 15. DOI.
- Zhang, X.J., Deng, L.H., Fei, Y., Li, C., Tian, X.A., Wan, Z.J.: 2022, Hemispheric asymmetry of long-term sunspot activity: sunspot relative numbers for 1939–2019. *Mon. Not. Roy. Astron. Soc.* **514**, 1140. DOI.

Publisher's Note Springer Nature remains neutral with regard to jurisdictional claims in published maps and institutional affiliations.

Authors and Affiliations

Partha Chowdhury¹ · Ali Kilcik²  · Ankit Saha³ · Jean-Pierre Rozelot⁴ · Vladimir Obridko^{5,6} · Robertus Erdélyi^{7,8,9}

✉ A. Kilcik
alilikcik@akdeniz.edu.tr

P. Chowdhury
parthares@gmail.com

A. Saha
ankit18saha@gmail.com

J.-P. Rozelot
Jean-Pierre.Rozelot@univ-cotedazur.fr

V. Obridko
obridko@mail.ru

R. Erdélyi
r.von.fay-siebenburgen@sheffield.ac.uk

- ¹ University College of Science and Technology, Chemical Technology Dept., University of Calcutta, 92, Acharya Prafulla Chandra Road, 700 009, Kolkata, India
- ² Department of Space Science and Technologies, Akdeniz University Faculty of Science, 07058, Antalya, Turkey
- ³ University College of Science and Technology, Chemical Engineering Dept., University of Calcutta, 92, AcharyaPrafulla Chandra Road, 700 009, Kolkata, India
- ⁴ Université de la Côte d'Azur (emeritus), 77 chemin des basses moulières, 06130 Grasse, France
- ⁵ Pushkov Institute of Solar–Terrestrial Physics, Ionosphere, and Radio Wave Propagation, Kaluzhskoeshosse 4, Troitsk, 108840 Moscow, Russia
- ⁶ Institute of Continuous Media Mechanics, Ural Branch, Russian Academy of Sciences, Academician Korolev Street 1, Perm 614013, Russia
- ⁷ Solar Physics and Space Plasma Research Centre, School of Mathematics and Statistics, University of Sheffield, Hicks Building, Hounsfield Road, Sheffield, S3 7RH, United Kingdom
- ⁸ Gyula Bay Petőfitér 3, Zoltán Solar Observatory (GSO), Hungarian Solar Physics Foundation (HSPF), Gyula, H-5700, Hungary
- ⁹ Department of Astronomy, Eötvös Loránd University, 1/A Pázmány Pétersétány, H-1117 Budapest, Hungary